Ecological Indicators 159 (2024) 111738

Contents lists available at ScienceDirect

Ecological Indicators

journal homepage: www.elsevier.com/locate/ecolind

Spatiotemporal dynamics of microbial communities and cyanobacteria blooms in two North American Lakes using long-read 16S rRNA sequencing

Manuel Castro Berman[a,b,*], Allison R. Hrycik[b,c], Angelica Costello[a], Yang Bai[a], Kevin C. Rose[b,c], Rick Relyea[a,b,c], Jonathan S. Dordick[a,b,c,d,*]

[a] Center for Biotechnology and Interdisciplinary Studies, Rensselaer Polytechnic Institute, Troy, NY 12180, United States
[b] Darrin Fresh Water Institute, Rensselaer Polytechnic Institute, Bolton Landing, NY, 12814, United States
[c] Department of Biological Sciences, Rensselaer Polytechnic Institute, Troy, NY 12180, United States
[d] Department of Chemical and Biological Engineering, Rensselaer Polytechnic Institute, Troy, NY 12180, United States

ARTICLE INFO

Keywords:
16S rRNA
Cyanobacteria blooms
eDNA
Lake George
Chautauqua Lake

ABSTRACT

Understanding spatial and temporal heterogeneity in ecosystems is essential to forecasting the effects of environmental changes. Freshwater microbes, including cyanobacteria, play a crucial role in food-web structures and biochemical processes, yet can exhibit substantial heterogeneity through space and time. They also act as powerful indicators of natural and human-induced stress due to their high metabolic and rapid response to environmental change. The formation of cyanobacteria blooms can be particularly important due to the potential production of toxins that are harmful to humans and wildlife. While high water temperatures and high nutrients are largely recognized as triggers of cyanobacterial bloom formation, there is growing evidence of the role of its associated microbiome in bloom formation. The inability to accurately forecast cyanobacteria blooms is challenged by uncertainty in the degree to which microbial diversity, and bloom forming taxa in particular, exhibit spatial heterogeneity and how spatial heterogeneity varies seasonally or between lakes spanning the trophic gradient. Here, we used long-read sequencing of the 16S rRNA gene to quantify variations in microbial spatiotemporal dynamics over the course of an ice-free season between two lakes that varied substantially in trophic status. Our results showed that the microbial community composition of eutrophic Chautauqua Lake was seasonally and spatially structured; however, during bloom events we observed lower diversity and a homogeneous community dominated by *Microcystis* and enriched with Gammaproteobacteria. In oligotrophic Lake George, seasonality rather than the basin of origin played a major role in structuring the microbial community; however, there was a significant difference between basins when controlling for the temporal effect and was linked to a South-to-North anthropogenic gradient. This study provides a solid foundation for exploiting long-read sequencing of prokaryotes and couples sequencing with traditional water quality monitoring to assess microbial dynamics (e.g., cyanobacteria bloom microbiome) and the effect of local and global stressors.

1. Introduction

Freshwater microbes play vital roles in lake ecology and are uniquely positioned as powerful indicators of natural and human-induced stress due to their rapid response to environmental changes (Caruso et al., 2016). Furthermore, changes in its community structure provide a more holistic representation of ecosystem variations compared to traditional physical and chemical monitoring programs (Cordier et al., 2021). Environmental DNA-based methods (e.g. amplicon sequencing) can offer insights into the trajectories of these microbes as sentinels of water quality (Sagova-Mareckova et al., 2021). While past constraints such as costly and lengthy protocols have hindered such approaches, recent advancements, including a relatively new molecular approach involving long-read sequencing (MinION^{TM}), make these methods more viable to couple to chemical and hydrological lake monitoring (Baird and Hajibabaei, 2012; Werner et al., 2022). This platform has been extensively used to identify microbes in mock communities and in clinical studies (Burton et al., 2020; Matsuo et al., 2021; Meslier et al., 2022; Rozas et al., 2022), but non-epidemiological studies in environmental research are still scarce (but see Koeppel et al., 2022).

---

* Corresponding authors at: Center for Biotechnology and Interdisciplinary Studies, Rensselaer Polytechnic Institute, Troy, NY 12180, United States.
E-mail addresses: castrm2@rpi.edu (M. Castro Berman), dordick@rpi.edu (J.S. Dordick).

https://doi.org/10.1016/j.ecolind.2024.111738
Received 9 November 2023; Received in revised form 7 February 2024; Accepted 9 February 2024

Changes in the microbial community, such as cyanobacterial blooms, can cause regime shifts from clear-water to turbid-water dominated by algae that can impose a substantial cost to local economies (Smith et al., 2019), disrupt ecosystems (Scheffer et al., 1993) and become toxic (Carmichael, 2001). Most cyanobacteria genera like *Dolichospermum* sp. and *Microcystis* sp. are capable of producing various kinds of toxins including cyclic peptides (e.g., microcystin) and alkaloids (e.g., anatoxin, saxitoxin, and cylindrospermopsin). They are also the most common producers of the taste- and odor-forming compounds geosmin and 2-methylisoborneol (MIB) found in surface waters (Jüttner and Watson, 2007). Despite the need for accurate identification and quantification of cyanotoxins, bioassays and chemo-analytical methods have a number of methodological pitfalls (e.g. the need of specialized training and expensive equipment) that pose serious constraints on routine field assessments. Furthermore, they are only applicable once the toxins are above a certain threshold. In contrast, molecular techniques have the capability to identify toxigenic cyanobacteria prior to the production and release of toxins into a water body (Al-Tebrineh et al., 2012). While not yet functioning as a standalone early warning system, these molecular analyses offer fundamental insights into bloom dynamics and potential toxicity. When combined with other monitoring methods, this data can play a vital role in refining predictive models and strengthening our overall preparedness for managing bloom events.

High nutrient loads and warm conditions are major drivers in cyanobacterial bloom development (Bogard et al., 2020; O'Neil et al., 2012; Tanvir et al., 2021). However, there is growing need to include the interactions between cyanobacteria and their associated microbiomes in cyanobacterial blooms studies (Pound et al., 2021). Specifically, heterotrophic bacteria can promote (Jiang et al., 2007) and suppress cyanobacterial growth (Gerphagnon et al., 2015). Moreover, *Microcystis* colonies were identified as hotspots for bacterial production and serve as a protected microhabitat where exchange of nutrients and carbon occur (Cai et al., 2014; Krausfeldt et al., 2017; Wang et al., 2021).

The patchy spatial and stochastic nature of blooms suggest that these processes are spatially heterogeneous and vary through time (Carpenter et al., 2020). Nevertheless, the transition to a constant bloom stage has been observed in changes in spatial indicators (e.g. spatial autocorrelation, skewedness, etc.) of state variables like pigments and biomass and has been proposed as early warning indicators under computational modeling (Buelo et al., 2018), field observations (Ortiz et al., 2020), and experimental settings (Butitta et al., 2017). Coincidentally, these studies documented an increase in spatial autocorrelation as systems approached a critical tipping point, potentially offering an early warning signal of the impeding shift to a bloom stage. While studies exploring changes in the spatial statistics of bacterial communities exist (e.g., Zhao et al., 2022), there is a scarcity of research exploring such changes in the context of cyanobacterial bloom. Therefore, identifying and tracking the dynamics of these specific bacteria while assessing changes in their resilience can be a valuable approach to integrate with chemistry biomonitoring for early bloom detection.

In this study, we followed the dynamics of the bacterial community composition in 12 nearshore basins in the oligotrophic Lake George (NY, USA) which is subjected to an anthropogenic impairment gradient, a rise in the water temperatures, and to the proliferation of ephemeral cyanobacterial blooms (Hintz et al., 2020; Reinl et al., 2023). We also identified and tracked the dynamics of the bloom-forming cyanobacteria and its associated microbiome along an eight-point transect in the eutrophic Chautauqua Lake (NY, USA) which undergoes recurrent cyanobacterial blooms. Additionally, we assessed cyanotoxin production potential by quantifying the abundance of genes associated with common cyanotoxins. We hypothesized that the specific bloom-forming cyanobacteria harbor a distinct bacterial microbiome, and that the spatial autocorrelation of these bacteria is higher during blooms and lower during clear-water conditions. Moreover, we predicted that spatial autocorrelation would be higher in the eutrophic Chautauqua Lake and lower in the oligotrophic Lake George. Specifically, the study addressed three research questions: (1) Can we use long-read sequencing of the 16S rRNA gene of prokaryotes to assess the identities and dynamics of bloom-forming cyanobacteria and their associated microbiome in Lake George and Chautauqua Lake? (2) Do these blooms have the potential to produce toxins in Chautauqua Lake and Lake George? (3) Can we use long-read sequencing of prokaryotes to capture the spatial and temporal structure of Chautauqua Lake and Lake George? Do we observe changes in the spatial structure of the microbial community composition and diversity during bloom events? We provide a comprehensive analysis of cyanobacterial dynamics, associated microbiomes, and the potential for toxin production, while also leveraging long-read sequencing technologies to enhance our monitoring methods for assessing environmental stressors and gain insight into the microbial communities in lake ecosystems.

2. Materials and methods

2.1. Study sites, sampling design and physical and chemical variables

The two-basin Chautauqua Lake (42.157, −79.398) is 28 km long and 3.2 km wide at its widest point, has a mean (maximum) depth of 9.1 (23) m in the North Basin and 4.7 (5.7) m in the South Basin. Early in the summer, Chautauqua Lake experiences dense cyanobacterial blooms from the genera *Microcystis, Aphanizomenon, Dolichospermum and Planktothrix* that usually extend into autumn, especially in the eutrophic, shallower and urbanized South Basin (Smith et al., 2020). In contrast, Lake George is a two-basin large lake (51 km long and maximum width of 3.3 km) with a mean (maximum) depth of 18 (58) m (Mather, 1939). This oligotrophic glacial lake has experienced an increase in water temperatures, orthophosphates and algal biomass over the past 37 years (Hintz et al., 2020). A slight phosphorus and chloride gradient has been observed as a result of widespread tourism activities and increasing human development (Hintz et al., 2020). Since the first reported algal bloom in 2020 (Reinl et al., 2023), Lake George has experienced more frequent autumn blooms, coincidentally in the more developed South Basin (Hintz et al., 2020).

Lake George was sampled monthly from April to October 2022 at 14 sites ($n = 97$) as part of a 40-year monitoring program aimed at capturing the growing season and assessing environmental changes (Fig. 1). Additional samples were collected from four opportunistic blooms along the shoreline of four basins in the southernmost part of the lake in late October (triangles in Fig. 1). Following a pilot survey in 2021 that revealed cyanobacterial blooms starting in early August and extending beyond the growing season, Chautauqua Lake was sampled every two weeks from August 8th to November 11th, 2022, at eight sites ($n = 56$) (Fig. 1). Additionally, five opportunistic blooms were collected along the shoreline throughout the sampling period (triangles in Fig. 1).

Twenty-two nearshore sampling sites were sampled, with an average distance from the shoreline of 585 ± 248 m for Chautauqua Lake and 144 ± 124 m for Lake George. We accessed these sites via motorboat during the daytime between mid-late summer and autumn for Chautauqua Lake and over the course of spring to autumn for Lake George. For all sampling, integrated water samples were collected in acid-washed polycarbonate bottles from the pelagic zone 30–40 cm below the surface. For bacterioplankton analysis, an average of 200 mL (Chautauqua Lake) and 430 mL (Lake George) of lake water was filtered through a 0.22 μm polycarbonate filter (Millipore), and frozen at −80 °C until nucleic acid extraction. Water temperature (°C), conductivity (S/cm), pH, dissolved oxygen (mg O_2 L^{-1}) and Blue Green Algae (BGA, μg L^{-1}) were collected following a 'spot' approach at a ~ 0.35 m depth at each sampling site using a calibrated handheld YSI EXO2 multiparameter sonde (Yellow Springs Instruments, Yellow Springs, OH), with an average collection time of 3:50 pm ± 2 h UTC for Chautauqua Lake and 3:15 pm ± 1.51 h UTC for Lake George. To understand the role of nutrients in the algal blooms, epilimnetic water samples were collected from each site for measurement of chlorophyll *a* (Chl-*a*), total

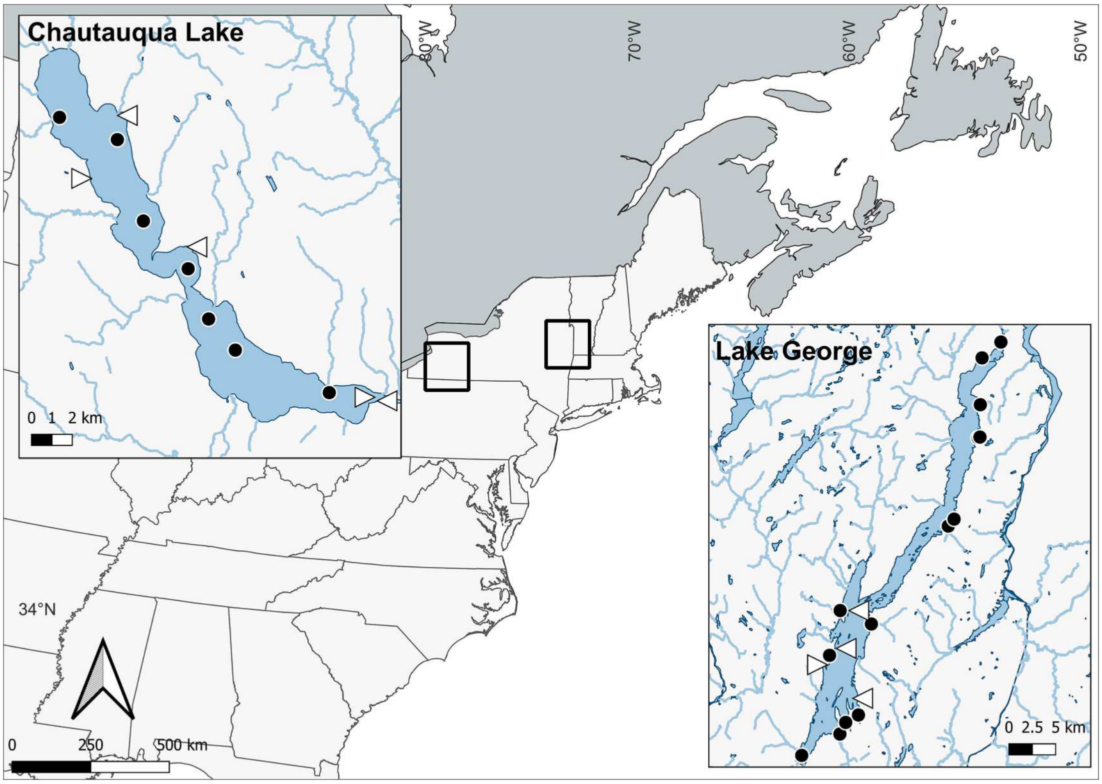

Fig. 1. Sampling locations in Chautauqua lake in Western New York State (NYS, USA) and Lake George in Eastern NYS. Monitoring samples are indicated by black dots while opportunistic blooms are indicated by vertex triangles.

phosphorus (TP), total dissolved phosphorus (TDP), soluble reactive phosphorus (SRP), nitrate (NO_3^-), total nitrogen (TN), total dissolved nitrogen (TDN), dissolved carbon (fDOM), sodium (Na), chloride (Cl^-), calcium (Ca), silica (Si) and iron (Fe), as described in Hintz et al. (2020). Chl-*a* and TP concentrations were used to calculate the Trophic Status Index (TSI) using the revised TSI proposed by Carlson (1977) while TN concentrations were used to calculate the TSI using Kratzer and Brezonik (1981) under nitrogen-limiting conditions.

2.2. *DNA Isolation, Sequencing, and analysis*

Genomic DNA was extracted using DNeasy PowerSoil Pro Kit (Qiagen, Germantown, MD) following the manufacturer's instructions with minor modifications including a 10-minute incubation step in warm (65 °C) lysis buffer and three bead-beading steps using a TissueLyser II (Qiagen, Germantown, MD). Concentration of eluted DNA was measured using a Qubit 4 Fluorometer with the Qubit™ dsDNA BR Assay Kit (ThermoFisher, Waltham, MA). Genomic DNA quality was checked by 2 % agarose gel electrophoresis (Bio-Rad, Hercules, CA) and stored at −20 °C prior to library preparation.

Sequencing libraries were prepared using 16S Barcoding Kit 1–24 (Oxford Nanopore Technologies -ONT-, Oxford, UK) and loaded into an R9.4.1 flow cell and sequenced on a MinION nanopore sequencer (ONT, Oxford, UK; RPI Genomics Research Core Facility). MINKNOW v22.10.10 including Guppy v6.3.9 (ONT, Oxford, UK) was used for sequencing data generation, de-multiplexing and read filtering by quality score of 7 and read length of 1300–2000 bp. We used the EPI2ME 16S workflow which uses the RefSeq NCBI 16S bacterial database to assign taxonomy; however, the software provides an output file that is not compatible for downstream analysis. Thus, sequence alignments were further conducted using minimap2 (Li, 2018) as recommended by Santos et al. (2020) against the SILVA database v-138-SSU-ref-NR-99 (https://www.arb-silva.de/documentation/release-138/). Additionally, we assessed the identity of cyanobacteria during blooms using the newly-curated Cyanoseq database (v1.2) (Lefler et al., 2023). During post-processing, the dataset was refined by excluding all mitochondria, chloroplast and eukaryote annotated features. Abundance tables for the different taxonomical ranks were parsed using in-house scripts in R (R-Core-Team, 2022). Sequences have been deposited at the European Nucleotide Archive (ENA) under the BioProject number (PRJEB67374).

2.3. *qPCR*

Genomic DNA was amplified via qPCR on a CFX96 thermocycler (Bio-Rad, Hercules, CA) with Phytoxigene^{TM} CyanoDTec Total Cyanobacteria kit (205–0050, Ohio, USA) to quantify cyanobacterial presence by targeting a universal sequence in the cyanobacterial 16S rRNA gene and The Toxin Gene kit for amplification of genes for microcystins/nodularins (*mcyE/ndaF*), saxitoxins (*sxtA*), and cylindrospermopsin (*cyrA*) production. These assays contain an internal amplification control to ensure that the qPCR reactions were not inhibited. We followed manufacturer's instructions for both reactions' preparation and thermal cycling conditions, Positive controls and non-template controls were included in every qPCR run. Finally, standard curves were created using the Phytoxigene™ CyanoNAS Nucleic Acid Standards (NA011-NA015).

2.4. *Classification of bloom stages*

Bloom conditions were defined as Chl-*a* exceeding 30 μg L^{-1}, as proposed by Bruns et al. (2022) following USGS guidelines. In addition to Chl-*a* concentration, we used a threshold of one or two standard deviations (SD) from the Chl-*a* peak at each site to define different stages in the bloom cycle. Smaller variations were considered as continuations of the bloom stage, depending on the context of each phenology curve. Pre-bloom (Eq. (1), early bloom (Eq. (2) and post-bloom (Eq. (4) stages were delineated based on sample dates preceding or following the Chl-*a* peak (Eq. (3). Chl-*a* concentrations greater than two SD below the peak was used to define no-bloom conditions (Eq. (5). Bloom duration, defined as days above the 30 μg L^{-1} Chl-*a* threshold, was determined by estimating the first and last days where Chl-*a* concentrations were over 30 μg L^{-1} while bloom intensity was defined as the maximum Chl-*a* concentration registered in that period.

$$\text{Pre-bloom} > 1\text{SD Chl-}a\text{ max} < \text{Chl-}a\text{ threshold} \tag{1}$$

$$\text{Early bloom} > 1\text{SD Chl-}a\text{ max} > \text{Chl-}a\text{ threshold} \tag{2}$$

$$\text{Bloom} < 1\text{SD Chl-}a\text{ max} > \text{Chl-}a\text{ threshold} \tag{3}$$

$$\text{Post bloom} > 1\text{SD Chl-}a\text{ max} > \text{Chl-}a\text{ threshold} \tag{4}$$

$$\text{No Bloom} < 2\text{SD Chl-}a\text{ max} < \text{Chl-}a\text{ threshold} \tag{5}$$

2.5. *Statistical analysis*

All statistical analyses were performed in R 4.1.3 and Rstudio (Rstudio Team, 2020). To explore environmental variation, we conducted a principal component analysis (PCA) using the 'pca' function from the *FactoMineR* package. Diversity indices of Bacterioplankton, including species richness, Chao1, Shannon-Wiener, and Pielou evenness, were calculated by bloom stage using *vegan.* We tested for significant differences using the Kruskal-Wallis rank sum test and performed multiple comparisons (Dunn's post hoc tests) with *rstatix*.

Non-metric Multidimensional Scaling (NMDS) analyses were performed on Bray-Curtis dissimilarity data (Hellinger transformed) using the metaMDS function from *vegan* to gain insights into changes in community structure during bloom stages. We considered only taxa accounting for more than 0.01 % of total abundance (Legendre and Gallagher, 2001). To assess the significance of spatial–temporal and bloom stages variations in community composition, we employed a one-way analysis of similarity (ANOSIM) as described by Clarke and Warwick, 1994. To highlight and validate the proposed bloom stages and identify discriminating components and features we utilized sparse partial least squares discriminant analysis (sPLS-DA) following the approach by Cao et al. (2016) with the *mixOmics* package. For identifying indicator taxa for each bloom stage based on their fidelity and relative abundance, we employed the Indicator Species Analysis (InDVal) using the 'multipatt' function in the *indicspecies* package. We only considered taxa with a significance level of $p < 0.05$ and IndVal values > 0.4, as recommended by De Cáceres and Legendre (2009).

To assess the influence of local environmental variables on the explained variation in the microbial community across all taxonomical ranks, redundancy analysis (RDA) was performed. The selection of variables for each model was carried out using the 'forward.sel' function in the *adespatial* package (Dray et al., 2009, $p < 0.01$, after 999 random permutations). We performed Mantel tests and Mantel correlogram to assess similarities between the community structure with the geographic distances and environmental factors. We calculated the geographic distance between lakes based on their coordinates. Additionally, we Z-score transformed the environmental variables and used them to calculate the Euclidean distance matrix. To assess changes in the spatial autocorrelation that could be used as predictors of a regime shift, we calculated Moran I on three categories: 1) diversity indices, 2) the bacterial composition, and 3) selected heterotrophic bacteria within each bloom stage. We generated a connectivity matrix based on Gabriel graph and a weighting matrix (lw) was calculated for each sampling point. Finally, we employed a Regularized Canonical Correlation Analysis (rCCA) to investigate the correlation between environmental variables and the microbial composition following Lê Cao et al. (2011).

3. Results

3.1. *Physical and chemical conditions*

Chautauqua Lake*.* The lake's trophic conditions ranged between meso- and eutrophic conditions. The South and Central Basin exhibited eutrophic conditions in 79 % of the samples (hereinafter both basins are grouped as South Basin), whereas the North Basin was mesotrophic in 74 % of the samples. On the other hand, 96 % of the samples showed TSI values for Total Nitrogen below 60 and over 40 indicating a mesotrophic condition accordingly with the observed low TN:TP ratios (<10) suggesting that the lake was nitrogen-limited during the period of this study (Table S1). During the summer, the South Basin had significantly higher levels of TP, Cl^-, TDN, TN, Si (Table S1) and higher values of Chl-*a,* Fe and turbidity during the autumn. The North Basin had higher SRP and TFP, along with higher Ca concentrations during the summer. Principal component analysis was used to visualize this complexity and revealed that the first two axes explained 61 % of the total variation (Fig. 2a). Trophic state variables (TN, turbidity, Chl-*a* and TP) characterized the first component which separated the South Basin from the North Basin (Fig. 2b), which was more clearly observed during the summer. Seasonal variables (e.g., water temperature, pH, Si, fDOM and Fe) and soluble nutrients that also showed a seasonal behavior (e.g., TDN, SRP and TDP) correlated with the second component resulting in a clear separation of summer from autumn samples (Fig. 2c).

Lake George*.* All samples indicated oligotrophic conditions for Chl-a, TP and TN, except for four mesotrophic samples that were collected closer to storm events in the South Basin. In contrast to Chautauqua Lake, during the study period, Lake George was more phosphorus-limited (TN:TP $>$ 10, Table S1). Most variables remained relatively constant and showed overlapping ranges throughout the sampling season within each Basin. In every sampling event, the South Basin had higher Cl^-, conductivity, fDOM, TN, TP (both total and dissolved) and Chl-*a* compared to the North Basin but differences were not significant (Table S1). The first two axes of the PCA explained 58 % of the total variation in Lake George (Fig. 2d) and the overlapping sites scores in the plot (Fig. 2e) reflected the similarities in environmental characteristics between basins. Major contributions of phosphorus (both filtered and total) and minerals (Fe and Si) characterized the first component, while the second component exhibited a correlation with seasonal variables such as DO, water temperature, conductivity, Cl^-, and Na and led to the separation of summer and autumn samples from spring samples (Fig. 2f).

3.2. *Microbial community composition and environmental variables*

Chautauqua Lake*.* The dataset consisted of 13,405,062 reads that were classified into 28 phyla, 55 classes, 121 orders, 187 families and 318 genera. The predominant bacterial classes were: Cyanobacteria (37 %), Gammaproteobacteria (25 %), Bacteroidota (11 %), Acidimicrobiia (4 %) and Verrucomicrobia (4 %). At the genus level, *Microcystis* PCC 7914 was the most abundant with an average value of 28 % throughout the entire sampling season; the highest values were recorded during mid-August through September (~63 %), followed by *Limnohabitans* and CL500-29 clade, which had similar abundances of ~ 4 % (Fig. 3a). The N_2-fixing cyanobacteria *Aphanizomenon* MDT14a and *Gloeotrichia PYH6* were also present early in the sampling season.

RDA (Table 1) revealed that, on average, 54 % of the variation could be explained by local environmental variables. The variables most frequently selected, with the highest individual R^2, were associated with water quality (e.g., turbidity) and specifically with cyanobacterial biomass (BGA). Water temperature explained approximately 12 % of the variation, while nutrients (e.g., TFP, SRP) and other physicochemical variables (Si and barometric pressure) explained a minor percentage of the variation. The Mantel test disclosed a similar trend, showing that cumulative environmental factors correlated with the microbial community composition (Mantel test r: 0.58, $p < 0.001$). Regularized

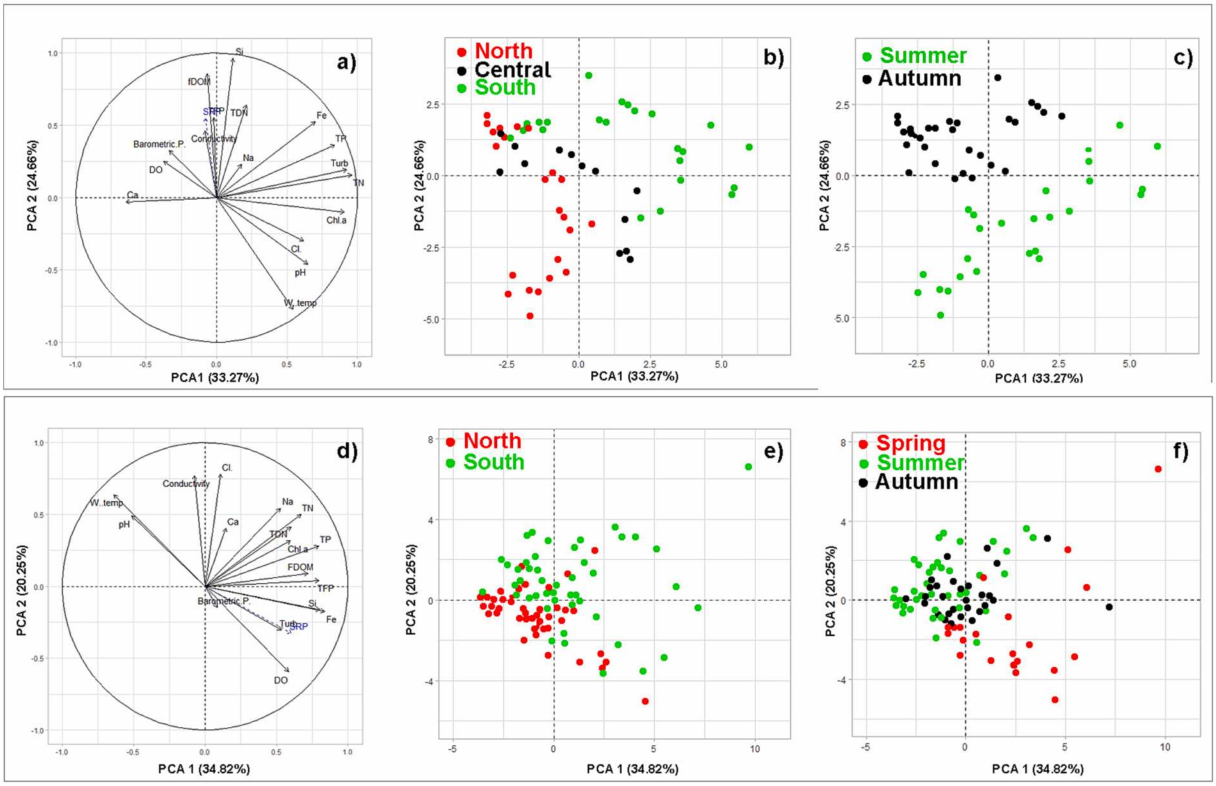

Fig. 2. PCA correlation plots of the environmental variables in Chautauqua Lake (upper panel) and Lake George (lower panel). (a, d) Loading plots of Chautauqua Lake and Lake George, respectively; (b, e) score plots of Chautauqua Lake and Lake George by Basin, respectively; and (c, f) score plots by season of Chautauqua Lake and Lake George, respectively.

canonical correlation analysis (rCCA) identified 114 genera with correlations > 0.50 and 10 environmental variables. Fig. 4a shows the heatmap of pairwise Pearson correlations among these selected variables and genera. There was a high proportion of genera that correlated positively (red) or negatively (blue) to high nutrients, low light quality, high water temperature and macronutrients (especially calcium) and a third group with intermediate correlations with these set of variables. The cyanobacterium *Microcystis* PCC 7914 showed a high and positive correlation with light quality (turbidity, TSS), TP, Fe, BGA, Chl-*a* and pH and a negative correlation with Ca, suggesting its contribution to the impairment of the water quality. The filamentous *Aphanizomenon* strain MDT14a only showed a positive correlation with water temperature while *Gloeotrichia PYH6* showed a negative correlation with turbidity. In general, taxa with an average abundance over 1 % (Fig. 3) except for the uncultured *Sutterelaceae* and *Ahniella* showed opposite correlations with environmental variables vs. that observed with *Microcystis* PCC 7914.

Lake George. The dataset consisted of 20,979,589 reads that were classified into 23 phyla, 42 classes, 106 orders, 171 families and 287 genera. The predominant bacterial classes and genera were: Gammaproteobacteria (44 %; e.g., *Limnohabitans*, *Polynucleobacter*), Alphaproteobacteria (18 %; e.g., *Candidatus Fonsibacter ubiquis*), Bacteroidota (14 %; e.g., Pseudarcicella), and Verrucomicrobia (6 %; e.g., uncultured Verrucomicrobiae) (Fig. 3b). The mean relative abundance of Cyanobacteria was low (0.2 % of total reads) and showed a seasonal dynamic with higher values (~7% of total class sequences) in late summer and early autumn. The picocyanobacteria *Cyanobium* PCC-6307 (black in Fig. 3b) was present throughout the 2022 sampling period with higher values in April and during the autumn while *Microcystis* PCC 7914 (orange) peaked in autumn and *Aphanizomenon sp.* NIES81 (pink) had the higher values in July. In four of the 101 samples, *Aphanizomenon sp.* NIES81 represented over 68 % of the total sequences.

RDA (Table 1) revealed that, on average, 32 % of the variation could be explained by local environmental variables. Water temperature emerged as the most frequently selected variable, explaining 20 % of the variation. On the other hand, nutrients (e.g., TFP), fDOM and other physicochemical variables (pH, Si and barometric pressure) each contributed to a minor percentage of the explained variation, averaging 5 %. The microbial community composition strongly correlated with cumulative environmental factors (Mantel test r: 0.50, $p < 0.001$) and rCCA analysis identified 51 genera and 14 environmental variables with a correlation value over 0.40 (Fig. 4b). Two communities exhibited a clear seasonal separation: one preferred warmer water temperature, and correlated with conductivity and pH (including the cyanobacteria *Microcystis* PCC 7914 and *Aphanizomenon* sp. NIES81), while the other group showed preference for cooler temperatures and high DO concentration (*CL500-29 clade*, *Candidatus Methylopumilus, hgcI clade*), as well as nutrients and fDOM (*Verrucomicrobiae, Pseudarcicella*). Despite the contrasting lake conditions in both lakes, most genera, including *Limnohabitans, Candidatus Methylopumilus, Rhodoferax, Microcystis* PCC 7914, *Aphanizomenon* NIES81, *Verrucomicrobiae* and *Limnobacter,* showed consistent correlation with water temperature and pH across this trophic gradient.

3.3. Spatial and temporal structure of the microbial community composition and diversity during bloom stages

Chautauqua Lake. A total of 48 % of samples met our definition of a bloom (≥30 μg L^{-1} Chl-*a*) with all sites experiencing a bloom stage (Fig. 5). 41 % occurred in the South Basin (Table S2), while 7 % occurred in the North Basin. During Chl-a peaks nearly all cyanobacteria sequences mapped to *Microcystis aeruginosa* PCC 7914 using minimap2 and the EPI2ME workflow, and to *Microcystis aeruginosa* PCC 7941 using minimap2 against the CyanoSeq database. The average (maximum) abundance of cyanobacteria 16S rRNA and *mcyE/ndaF* copies were 2.58 $\times 10^5$ L^{-1} (3.97×10^6 L^{-1}) and 4.60 $\times 10^4$ L^{-1} (9.49×10^5 L^{-1}), respectively. The *cyrA* gene was not detected, while the *sxtA* gene for saxitoxin

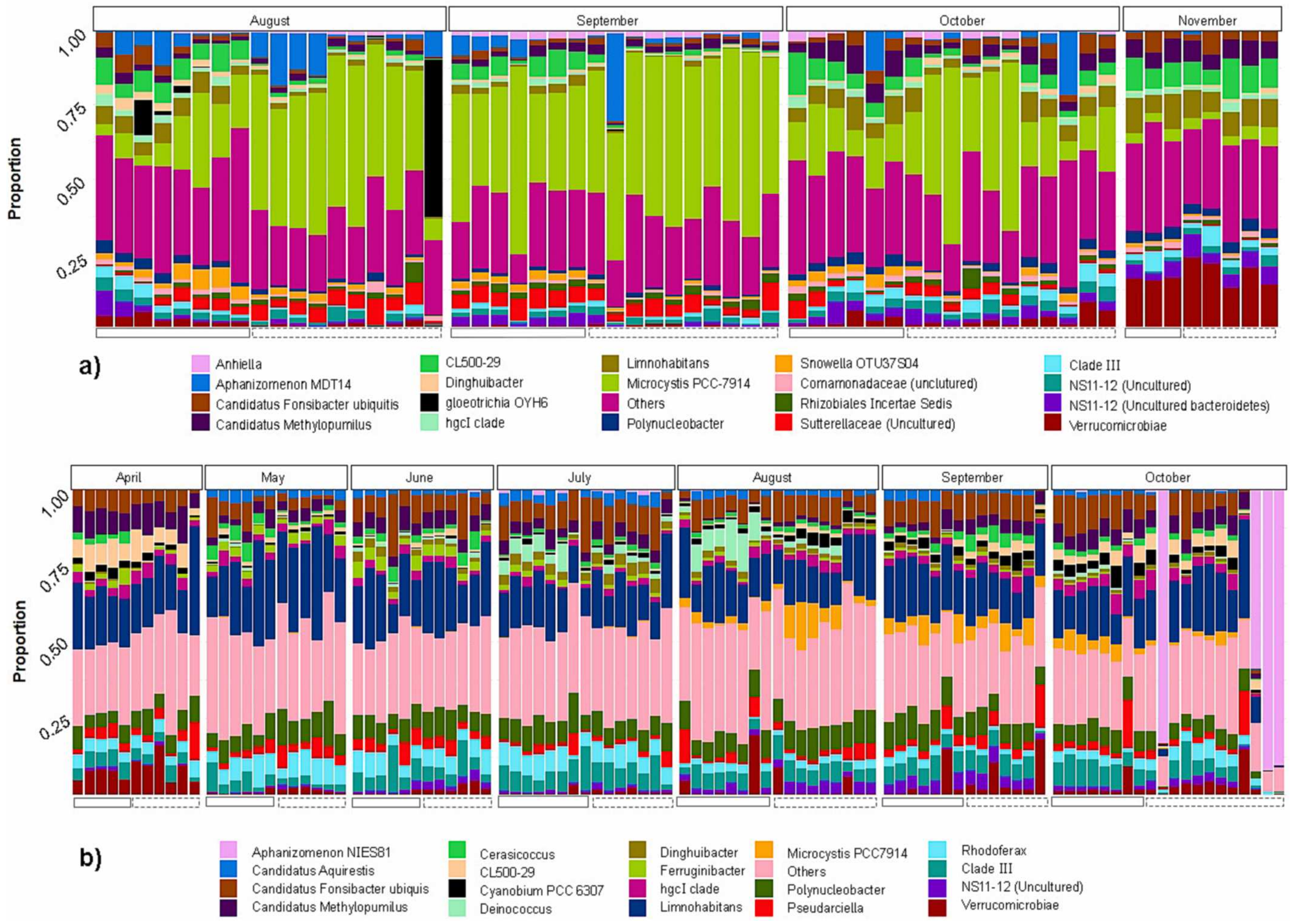

Fig. 3. Relative abundance of bacteria genera that accounted for 70% of total sequences in (a) Chautauqua Lake and (b) Lake George in the South Basins (⬚) and North Basins (□).

Table 1
Redundancy Analysis (RDA) showing the individual R^2 for each selected environmental variable and total adjusted cumulative R^2 for Chautauqua Lake and Lake George across all taxonomic ranks.

	BGA	Water temp.	fDOM	TFP	Si	Turbidity	SRP	pH	B. pressure	R^2_a
Chautauqua Lake										
Phylum	0.46	0.11					0.04			0.59
Class	0.43	0.11		0.03						0.54
Order		0.14		0.05		0.34				0.50
Family	0.34	0.11			0.07					0.49
Genus		0.16				0.34	0.06		0.04	0.56
Lake George										
Phylum		0.19		0.08	0.04	0.05				0.32
Class		0.19	0.07					0.04		0.26
Order		0.19	0.07		0.03			0.04		0.30
Family		0.21	0.06	0.04	0.04			0.04	0.03	0.37
Genus		0.21	0.06	0.04	0.04			0.05	0.03	0.37

Only variables with a $p < 0.01$ are shown.

production was detected once (Table S2). The *mcyE/ndaF* gene was at least one order of magnitude lower than the 16S rRNA, yet it was consistently present and its ratio ranged from 0.02 to 44 % (average 8 %) with higher values observed during the summer. *mcyE* and 16S strongly correlated with each other (r (48) = 0.95, p = <0.05), and with turbidity and BGA (r (48) > 0.79, p = <0.05), indicating their presence within *Microcystis* cells and its contribution to the water quality of the lake.

The most significant sources of variation on the microbial composition were season (ANOSIM R: 0.50, $p < 0.001$), sampling event (ANOSIM R: 0.54, $p < 0.001$) and basin of sample origin (ANOSIM R: 0.22, $p < 0.001$), with a clearer basin separation during the summer (ANOSIM R: 0.49, $p < 0.001$). Chl-*a* concentrations and bloom stages also played a substantial role in shaping the microbial composition. At the beginning of the sampling season, a brief pre-bloom occurred in the North basin while the South Basin was already in a bloom stage. This period exhibited the highest dissimilarities in the microbial composition between basins (ANOSIM R: 0.82, $p < 0.05$, Fig. 5a). When blooms developed in the North Basin the microbial community became more

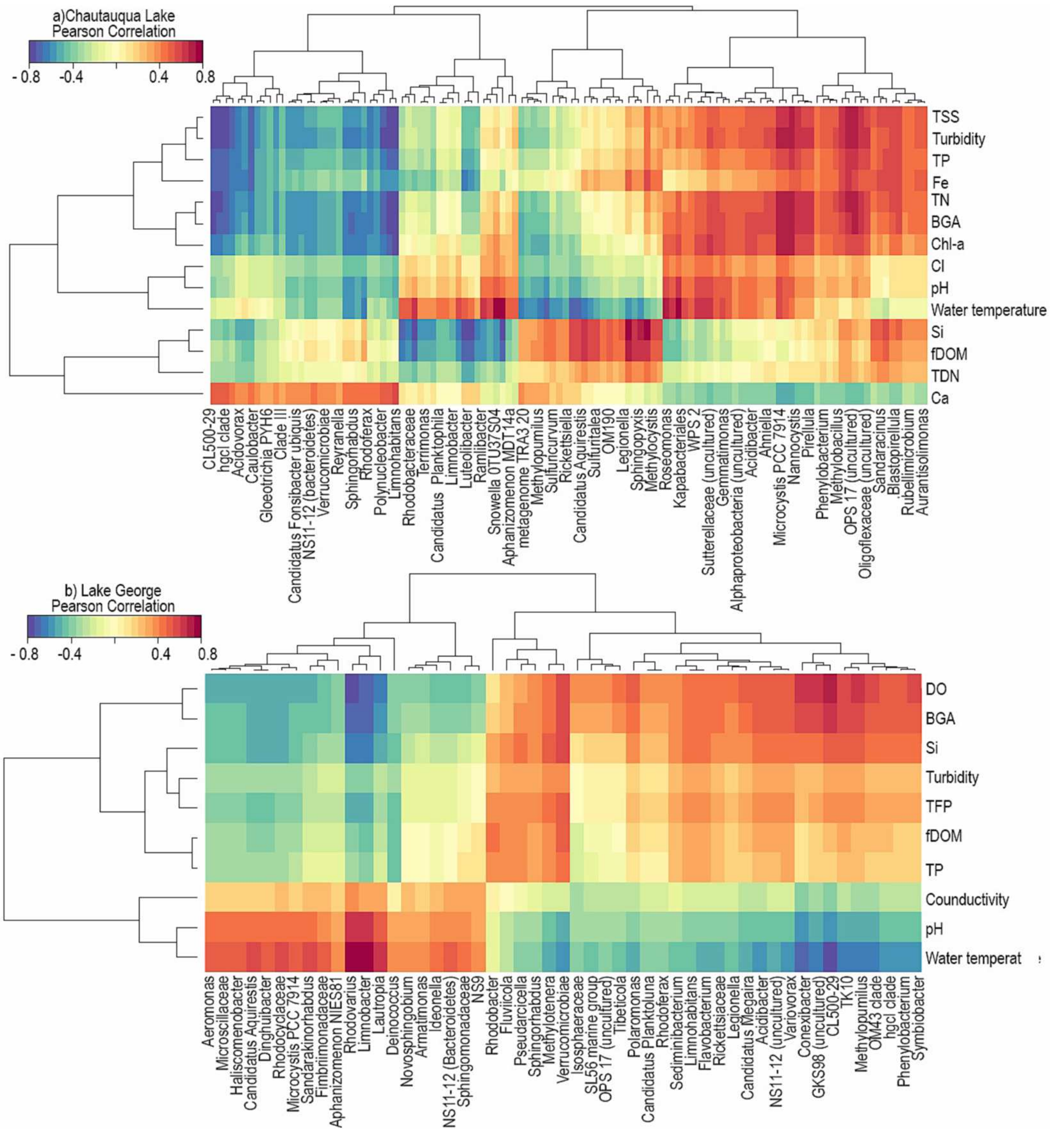

Fig. 4. Heatmap depicting correlations among the selected genera and nutrients according to rCCA analysis of the bacterial communities and environmental variables in (a) Chautauqua Lake and (b) Lake George. Red and blue denote positive and negative association, respectively. (For interpretation of the references to colour in this figure legend, the reader is referred to the web version of this article.)

similar to that of the South Basin (Fig. 5b and Fig. 5c). Later, Chl-*a* concentrations in the North Basin sharply decreased and remained low and in a no bloom stage until the end of the season. Meanwhile, in the South Basin, Chl-*a* concentrations gradually declined entering a post-bloom stage where significant differences in microbial composition between the basins were still evident (Fig. 5d and Fig. 5e). However, as Chl-*a* levels decreased and reached similar concentrations to those of the North Basin, the grouping by basin of origin became less clear (Fig. 5f and Fig. 5g).

Pre-bloom stages had a similar composition to the four blooms observed in the North Basin, while the three early blooms were similar to the blooms in the South Basin (ANOSIM $p > 0.05$). Thus, we treated them as a single bloom stage consisting of early bloom, pre-bloom and bloom (n: 25). The sPLS-DA analysis supported the bloom classification proposed here: bloom and no-bloom stages formed two tight clusters with few mismatches, while the post bloom stage had higher overlapping samples showing the transitional nature of this stage (average cross validation error rate for the first component was 0.22 and 0.13 for the second component) (Fig. S1a). Species richness and Chao1 estimator were lower during the bloom stage (Dunn's $p < 0.05$), while the no bloom stage had higher Shannon-Wiener and Pielou evenness. The indicator value index (IndVal) revealed that genera belonging to Gammaproteobacteria were characteristic of the bloom stage (Table 2). Genera belonging to the phyla Myxococcota and Planctomycetota were indicators of post bloom stage and Actinobacteriota, Bacteroidota and Chloroflexi were characteristic of the no bloom stage.

The proportion of bacteria with positive and significant Moran I ranged from 0.09 to 0.47. After a sharp drop on August 8th, it gradually increased towards late summer and declined as Chl-a concentrations decreased (Fig. 6a). In contrast, Moran I values for Chl-a exhibited one peak on September 12th, before the North Basin's transition to a no bloom stage, and another one on October 25th when the entire lake was in a no bloom stage. Mean Moran I value for these bacteria ranged from 0.46 to 0.65 (Fig. 7a), revealing a subtle "humped" pattern, with values gradually increasing towards the summer and decreasing afterwards, and showing high overlap among adjacent sampling event. The Mantel correlogram indicated that the observed spatial autocorrelation was significant at the first distance class, suggesting that closely located sites tended to show similar composition and diversity. However, Moran I of the indicator species within each bloom stage showed a similar pattern

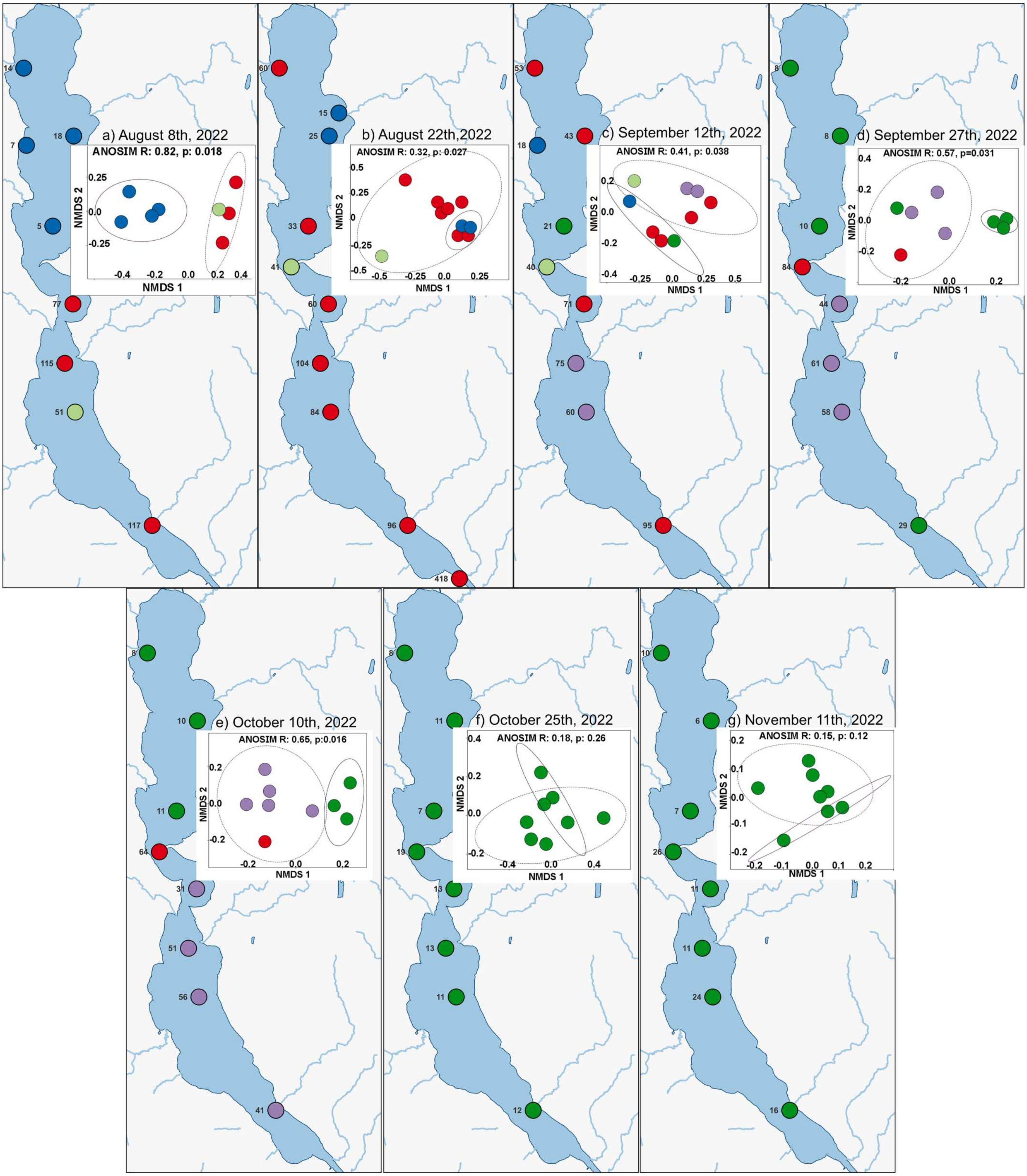

Fig. 5. Chl-*a* concentrations and bloom stages in Chautauqua Lake during pre-bloom (●), early bloom (●), bloom (●), post bloom (●) and no bloom (●) stages from August (a) to November (g). Ordination diagram for Non-metric Multidimensional Scaling (NMDS) as well as the ANOSIM R test values comparing the microbial communities Bray-Curtis differences are showed for each sampling event. Chl-*a* values is labeled next to each sampling point.

to that of the entire microbial distribution (Figure S2, $p > 0.05$). Moreover, no indicator species showed significant Moran I in all sampling events hindering the potential to be used as an early warning to a regime shift.

Lake George. The most significant sources of variation on the microbial composition were sampling event (ANOSIM R: 0.75, $p < 0.001$) and season (ANOSIM R: 0.61, $p < 0.05$). The influence of the basin of sample origin was only clear when considering sampling events individually (Fig. 8). These differences were particularly pronounced during the autumn, specifically in the months of September and October

Table 2
Taxa identified at the dominant genus levels as potential indicators from taxa analysis of the three post hoc groups in Chautauqua Lake and Lake George.

Bloom stage	IndVal	P value	Taxon
Chautauqua Lake			
Bloom	>0.4	<0.05	Gammaproteobacteria*: B63, Noviherbaspirillum, Sphaerotilus, Comamonas, Silanimonas*
Post Bloom	>0.5	<0.05	Alphaproteobacteria*: Sphingopyxis, uncultured alphaproteobacteria, Rubellimicrobium, Methylocystis;* Gammaproteobacteria: *Ahniella, BD1-7 clade, MND1;* Myxococcota*: P3OB, Sandaracinaceae, Sandaracinus, mle1.27, Nannocystis;* Planctomycetota*: Blastopirellula, OM190*
No Bloom	>0.5	<0.05	Alphaproteobacteria*: Cereibacter, Reyranella, Sphingorhabdus;* Gammaproteobacteria*: Rhodoferax, Methylopumilus, Limnohabitans, GKS98, Oxalobacteraceae, B1-7BS;* Actinobacteriota*: CL500-29;* Bacteroidota*: Fluviicola, Sediminibacterium, NS11-12;* Chloroflexi*: SL56*
Lake George			
Bloom	>0.5	<0.05	Cyanobacteria*: Aphanizomenon NIES81;* Alphaproteobacteria*: Sphingorhabdus, Phenylobacterium, SM2D12, Massilia, Caulobacter, alphaI cluster;* Gammaproteobacteria*: Acidovorax*

IndVal, Indicator Value, the association between species and sampling groups with a permutation test.

(Fig. 8f and Fig. 8g). It is worth mentioning that two sites, Ticonderoga (located at the final discharge point of the lake in the North Basin) and Warner Bay (situated in a highly developed area in the South Basin), exhibited the highest Bray-Curtis distance when compared to the other sites. The exclusion of these sites enhanced the grouping by sampling event (ANOSIM R: 0.88, $p < 0.01$), season (ANOSIM R: 0.70, $p < 0.01$) and basin of sample origin specially in the months of September (ANOSIM R: 0.92, $p < 0.01$) and October (ANOSIM R: 0.83, $p < 0.01$). On the other hand, we observed no significant differences ($p > 0.05$) in the diversity indices between basins in any sampling event.

The microbial composition of the four autumn blooms showed significant differences with the no-bloom samples collected in that timeframe at all taxonomic ranks (ANOSIM R > ~ 0.90, $p < 0.001$), and also exhibited significant lower diversity indices values ($p < 0.05$). Most *Aphanizomenon* reads (pink in Fig. 3) mapped to *Dolichospermum* (NCBI: txid748770) using the EPI2ME workflow and to *Dolichospermum lemmermannii* (NCBI: txid1927882) using minimap2 against the CyanoSeq database. The average (maximum) abundance of cyanobacteria 16S rRNA was 2.95 × 105 copies L − 1 (5.42 × 105 copies L − 1) while the *mcyE/ndaF*, *cyrA* and *sxtA* were not detected. The sPLS-DA analysis (average CV first component error: 0.28, second component: 0.06 and third component: 0.04), supported a clustering by season and blooms events (Fig. S1b). The indicator value index (IndVal) revealed that the heterotrophic bacteria *Sphingorhabdus*, *Lacibacterium aquatile*, *Acidovorax*, *Phenylobacterium* and the uncultured bacterium SM2D12 showed the highest association values during these bloom events (Table 2).

The proportion of bacteria with positive and significant Moran I ranged from 0.10 to 0.49. This proportion displayed a skewed distribution towards the summer, with lower values in the spring and decreasing towards the autumn (Fig. 6b). Moran I for these bacteria ranged from 0.42 to 0.55 and were significantly lower than in Chautauqua Lake (Fig. 7b). There was high overlap among adjacent sampling events with no clear trend. The Mantel correlogram consistently showed significant and positive correlation at the smaller distance class at all sampling events except for October 18th. Moran I value of the bloom indicator taxa were similar to those of the whole community and to those assigned to no group (Figure S3). No bacterial genus showed consistent spatial correlation throughout the season that could be used as an early warning of a regime shift. Finally, we observed no significant spatial autocorrelation for Chl-a, which is consistent with the little variation in Chl-a and the localized, sparse and ephemeral nature of the reported bloom events (Table S2).

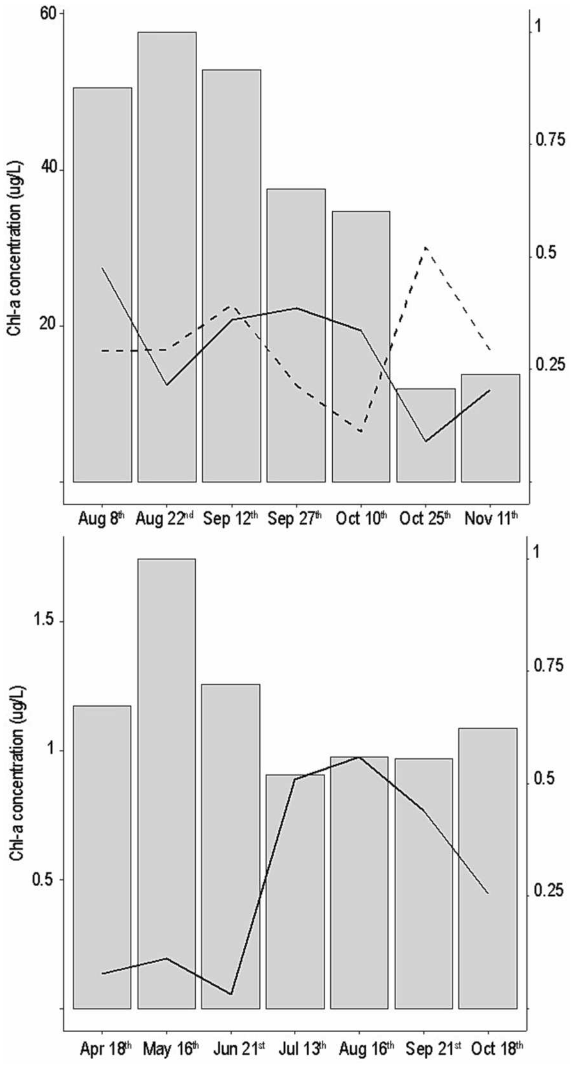

Fig. 6. Chl-a concentration (bars), and Chl-a Moran I correlation values (dashed) and proportion of bacteria (solid line) with positive and significant Moran I in Chautauqua Lake (upper panel) and Lake George (lower panel).

4. Discussion

The subsequent discussion is structured around the three questions posed in the introduction section: Subsection 4.1) Can we use long-read sequencing of the 16S rRNA gene of prokaryotes to assess the identities and dynamics of bloom-forming cyanobacteria and their associated microbiome in Lake George and Chautauqua Lake?; Subsection 4.2) Do these blooms have the potential to produce toxins in Chautauqua Lake and Lake George?; Subsection 4.3) Can we use long-read sequencing of prokaryotes to capture the spatial and temporal structure of Chautauqua Lake and Lake George? Do we observe changes in the spatial structure of the microbial community composition and diversity during bloom events? In the following subsections, we develop our interpretation of the results framed within the above three questions.

4.1. Long-read sequencing of the 16S rRNA gene of prokaryotes during cyanobacterial blooms

Classification of 16S rRNA gene reads using curated databases often

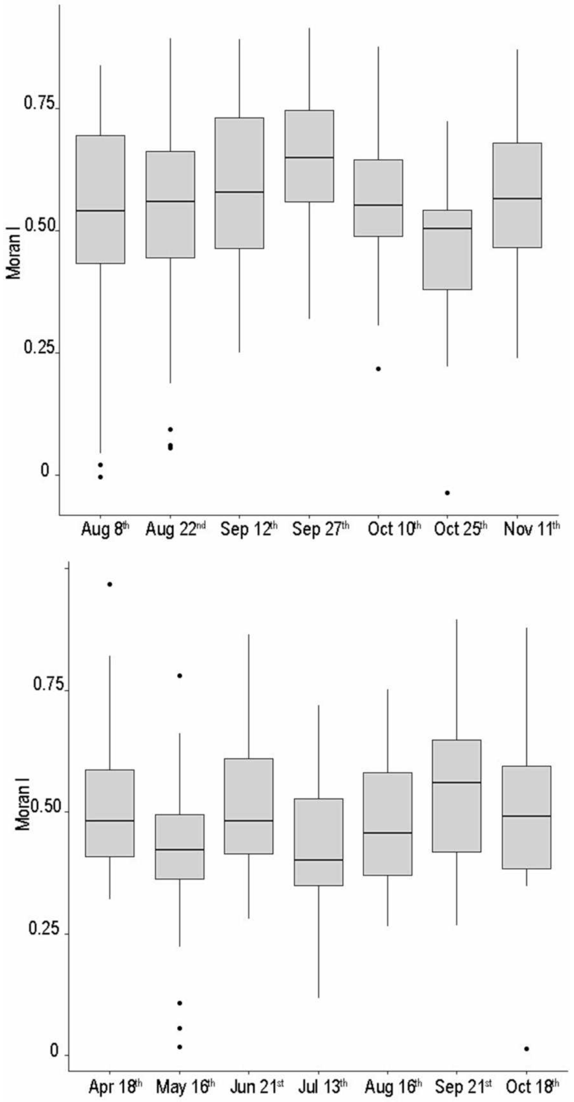

Fig. 7. Spatial indicator (Moran I) calculated for each bacteria genus with over 0.01 % contribution to total abundance in Chautauqua Lake (upper panel) and Lake George (lower panel).

encounters difficulties in assigning taxonomy to cyanobacterial reads due to the frequent changes in its lineages and taxonomy (Lefler et al., 2023). For example, members of the genus *Anabaena* with gas vesicles and planktonic habitat were reclassified as *Dolichospermum* (Wacklin et al., 2009). This was the case for Lake George' blooms, where most sequences mapped to *Dolichospermum* in the NCBI (NCBI:txid748770) and CyanoSeq (NCBI: txid1927882) databases, while they were mapped to *Anabaena* sp. *90* in the SILVA database (Wang et al., 2012). Although these hurdles are not specific to long-read sequencing and also exist for short-reads sequencing technologies, a "polyphasic" approach that incorporate and combines morphology-based with genetics, among other features (ecology, toxin production, etc.), is highly encouraged (Komárek, 2016). Regarding the use of long-read sequencing technologies for genomic-based monitoring, to our knowledge, only Koeppel et al. (2022) used MinION for the identification of cyanobacteria in a set of bloom samples from Lake Erie. Nonetheless, despite being a limited dataset (n: 10), the authors successfully identified the bloom-forming cyanobacteria and two potential heterotrophic bacteria that could be indicators of a microbial shift preceding the bloom. Limited by bioinformatics analysis, specifically the lack of methods for Operational Taxonomic units (OTU) picking and Amplicon Sequence Variants analysis (ASV) for nanopore data (Santos et al., 2020), MinION nonetheless proves valuable for its affordability, quick library preparation and rapid sequencing runs (∼48hs). These advantages make it well-suited to capturing clear signals and the local factors influencing the dynamics of the microbial communities across diverse physical and chemical conditions.

The bloom of a dominant species is considered a drastic environmental disturbance and has been usually associated with a lower diversity of phytoplankton (López-Archilla et al., 2004), zooplankton (Bockwoldt et al., 2017) and bacterial communities (Yang et al., 2021). In this study we found that α-diversity and evenness was lower during the bloom and post-bloom stages, but the species richness during the post-bloom stage was similar to that of the no-bloom stage, reflecting the high resilience of the microbial communities after the initial disruption. Cyanobacterial blooms can disrupt the microbial community structure but may also rely on the functions such communities may provide. In this sense, Cook et al. (2020) proposed that the microbiome associated with *Microcystis* blooms shares a similar composition, phylogeny and biochemical function at a global scale. Consistent with this proposition, we observed a taxonomically conserved bacterial composition during blooms in both lakes as supported by the ordination and machine learning approaches.

Blooms were dominated by *Microcystis* in Chautauqua Lake and by *Anabaena/Dolichospermum* in Lake George. Although its microbiomes were not compositionally identical, they showed a remarkable functional similarity. For instance, Lake George blooms were enriched with Alphaprotebacteria with bioremediation properties for cyanopeptides and cyanotoxins like *Sphighordhabdus*, which is novel to co-occurred with *Anabaena/Dolichospermum* in natural samples, and *Phenylobacterium, Massilia* and *Caulovacter* that can track organic compound gradients and capitalize it in this patchy environments (Pernthaler, 2017). In Chautauqua Lake, blooms were enriched with copiotrophs of Gammaproteobacteria, which are abundant in the proposed global *Microcystis* interactome (Cook et al., 2020). During the post-bloom stage, indicator species were associated with bloom decomposition (e.g., *Sphingopyxis, Anhiella*; Mankiewicz-Boczek & Font-Nájera, 2022; Sharma et al., 2021), phytoplankton exudates (Wang et al., 2022) and carbohydrate degradation (e.g. *Sandaracinus and unidentified Sandaracinaceae*; Sharma et al., 2016). During the no-bloom stage, we observed the coexistence of good-quality water indicators such as Oxalobacteraceae, NS11-12, *Sediminibacterium* and *Fluviicula,* which can also inhibit *Microcystis* growth (Guo et al., 2020*)*, along with bad quality indicators found in sludge (e.g., *Rhodoferax;* Hu et al., 2021) and impaired environments (e.g., *Reyranella;* Cui et al., 2017*)*.

4.2. Toxin production potential

We further enhanced the accuracy and resolution of our environmental genomic-based approach by assessing the abundance of cyanotoxins genes and total cyanobacteria. Distinguishing toxigenic populations is as critical as identifying the causes and identities of a bloom. In this sense, a strain similar to the one found in Lake George was recently linked to the death of 32 steers in southeastern Oregon (U.S.) (Dreher et al., 2019). However, this was not the case in Lake George, where no toxigenic genes or cyanotoxins were detected (Dr. Jacob Shelley personal communication) and there were no reports of human or animal exposure. On the other hand, we detected the *mcyE* gene which is required for microcystin production in all Chautauqua Lake samples. The presence of the *sxtA* gene supports the need to adopt a more thorough cyanotoxin monitoring program that does not solely focus on microcystin (Brown, 2022). Cyanotoxins are complex and expensive secondary metabolites that have been suggested to be associated with higher nutrient requirements in toxin strains compared to non-toxic strains (Lee et al., 2000). Accordingly, we found that the *mcyE*/16S rRNA ratio was similar to that reported in other eutrophic lakes (0–37 % in Hotto et al., 2008 and 0.7–41 % in Ha et al., 2009). Brown (2022)

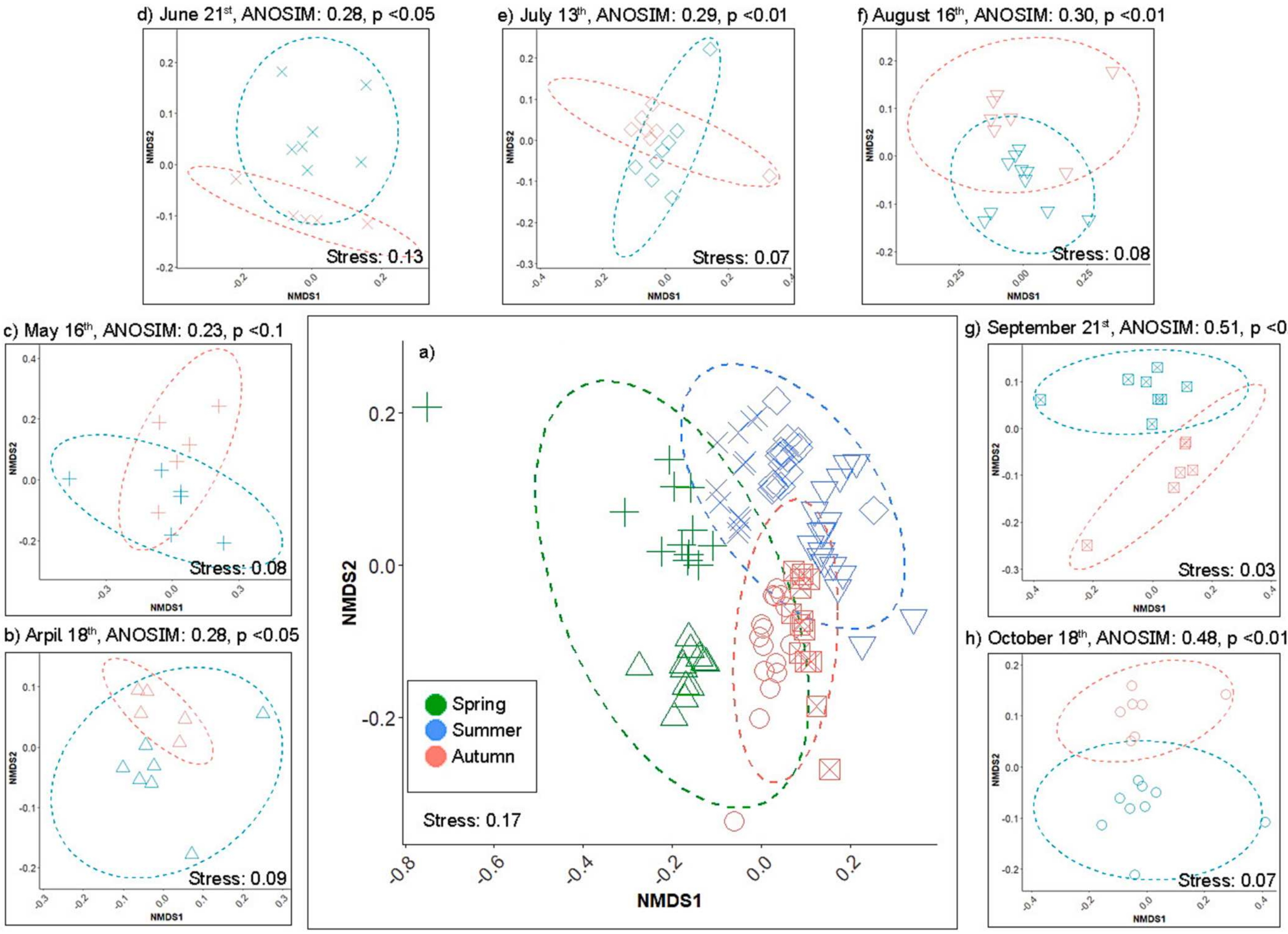
d) June 21st, ANOSIM: 0.28, p <0.05

e) July 13th, ANOSIM: 0.29, p <0.01

f) August 16th, ANOSIM: 0.30, p <0.01

c) May 16th, ANOSIM: 0.23, p <0.1

g) September 21st, ANOSIM: 0.51, p <0.01

b) Arpil 18th, ANOSIM: 0.28, p <0.05

h) October 18th, ANOSIM: 0.48, p <0.01

Fig. 8. Ordination diagram for Non-metric Multidimensional Scaling (NMDS) and ANOSIM test values used to compare Bray-Curtis differences in microbial communities between the Lake George's South (●) and North (●) Basins during spring (●), summer (●) and autumn (●) for the months of b) April (Δ), c) May (+), d) June (x), e) July (◇), f) August (▽), g) September (☒) and h) October (o), center figure (a) shows all Lake George samples plotted together for a better visualization of the temporal pattern.

observed concentrations of microcystin in Chautauqua Lake that spanned a wide range (0.04–1.0 μg L^{-1}) for the same number of *mcyE* copies, suggesting that monitoring these genes should be paired with expression profiles and detailed toxin analysis.

4.3. Spatial and temporal community structure

In contrast to single fixed-location schemes, often conducted over the deepest point, our multi-location approach allowed us to capture the spatial heterogeneity of both lakes in each sampling event. In Chautauqua Lake, the microbial community structure was influenced by the bloom cycle. For instance, during the bloom stages in late summer, the differences between the basins became less clear, and we observed a slight homogenization of the lake. However, the presence of filamentous N2-fixing cyanobacteria (*Aphanizomenon* MDT14a and *Gloeotrichia* PYH6), particularly during the first sampling events, suggests the presence of succession patterns between N2-fixing and non-diazotrophic organism before our sampling began. This succession pattern is well-studied in experimental settings (McDonald and Lehman, 2013; Paerl and Otten, 2016; Wu et al., 2016) and field settings (Tanvir et al., 2021). In many cases, it was observed to exhibit anticorrelation (Miller et al., 2013) and of particular importance in nitrogen-limited lakes such as Chautauqua Lake (Paerl et al., 2020a, 2020b). Interestingly, after the Chl-*a* drop to a no bloom stage in the Autumn, the grouping by basin became less clear despite the large environmental differences between Basins (Smith et al., 2020). Cyanobacterial blooms can trigger bacterial succession patterns (Eiler and Bertilsson, 2004; Niu et al., 2011) and *Microcystis* was found to be among the main lines for succession in lake sediments which suggest that once the bloom occurred it may trigger successional patterns that may persist beyond the growing season (Zhu et al., 2019). Local environmental variables explained a substantial (>50 %) portion of the microbial variation; however, it cannot be excluded that these variables are themselves spatially structured and influenced by land use within the watershed. In Chautauqua Lake, for example, agriculture encompasses 22 % of the watershed and contributes an estimated 7,500 kg of the total 20,500 kg annual phosphorus load (Stainbrook et al., 2022). Agricultural practices, particularly intensive ones, are well-documented in their promotion of algal biomass (Sánchez et al., 2023) and cyanobacterial abundance (Castro Berman et al., 2022, 2020).

Lake George's physical and chemical conditions have largely remained unchanged and in an oligotrophic state for decades (Hintz et al., 2020). Nonetheless, water temperature raised 1.8 °C over a 37-year period from 1980 to 2016 (Hintz et al., 2020) and it was consistently selected in the RDA analysis as the main predictor of microbial variation. Accordingly, we observed a clear seasonal structure, and the microbial composition clustered following their water temperature preferences. For instance, the bloom-forming *Aphanizomenon* sp. NIES81 showed a positive correlation with water temperatures, and the four bloom events could be linked to the longer growing season (Swinton et al., 2015). Close to the beginning of that temperature increase, Methe et al. (1998) found that the bacterial communities in the lake were dominated by Betaproteobacteria (now Gammaproteobacteria) and Alphaproteobacteria in a similar abundance as reported here. Nonetheless, the limited taxonomic resolution and variations in sequencing technologies and databases hinder our ability to examine potential changes at lower taxonomic ranks.

Lake George is also experiencing a slight chloride and nutrient gradient as a result of the increasing urban development and road salt contamination (Hintz et al., 2020). Accordingly, we observed higher chloride and nutrients concentrations in the South Basin at all sampling events, and the microbial composition reflected significant dissimilarities when considering only samples collected in the same sampling event. While dispersal from riverine communities and storm events (Adams et al., 2014) could have promoted some of these dissimilarities, environmental habitat characteristics is suggested to be the predominant mechanism structuring the microbial composition in lakes with long retention times, such as Lake George (Adams et al., 2014; Lindström and Bergström, 2004; Logue and Lindström, 2010). This observation was further supported by the significant co-variation observed between local environmental variables explaining 30 % in the 16S rRNA community structure as revealed by the RDA analysis. On the other hand, Ruka et al. (2022) reported that the south to north anthropogenic gradient observed in Lake George promotes the growing of small centric diatoms during the summer in the South Basin. While we did not explicitly assess land use variables, such as urbanization, there was a large proportion of unexplained variation in the RDA analysis that could be associated to spatially structured human activities as reported by Ruka et al. (2022).

Spatial statistics are proposed as promising tools to study cyanobacterial blooms as they faithfully reflect the ecosystem state and can provide a classification of bloom stages from a single spatial snapshot (Buelo et al., 2018). Moran I was observed to increase or decrease towards a critical transition, depending whether the bloom is rising or falling (Butitta et al., 2017). Accordingly, in Chautauqua Lake, we observed that the spatial autocorrelation of Chl-a concentration rose prior the transition to the no bloom stage in September 12th, almost a month earlier, and it rose again when the entire lake transitioned to a no-bloom stage. On the context of lake management, bloom collapse can be linked to the release of intracellular toxins, as observed during the 2014 and 2019 water crisis in Toledo (USA; McKindles et al., 2020). Spatial asymmetry has been reported before but in an opposite trajectory: higher values, closer to 1, were observed during a constant bloom state rather than to the no bloom stage (Buelo et al., 2018). However, the high asynchronicity in bloom development, where geographically close sites have large differences in Chl-a concentration, poses a complication in the interpretation of early warnings at this lake-wide scale. Finally, phytoplankton may not be the only source of Chl-*a* in the ecosystem (e.g., macrophytes), and living organisms such as prokaryotes, could be used to predict ecosystem transitions as well. Here, we observed that both the proportion of bacteria with significant and positive autocorrelation and the Moran I values were higher during September 27tt, that is one sampling event later the first peak in Chl-a autocorrelation. While bacteria have short generation times, that enable them to quickly react to variations in the environment, this could suggest a delay between stress signal which is the rise in Chl-a to a bloom stage and the response of the microbial composition.

5. Concluding remarks

In this study, we couple an environmental genomics approach with Lake George's long-term monitoring program to represent its ecology in line with recent reports on water warming and the anthropogenic impairment gradient. Due to limited information on bacterial communities in Lake George, we compare it with reports on other biological groups and to a hybridization-based sequencing study from almost 30 years ago. This underscores this study's importance as a benchmark for bacterial research and impairment assessment in Adirondack lakes, and supports the need to build robust and consensual methodological standards for the routine adoption of the e-DNA-based approaches in water quality monitoring programs (Cordier et al., 2021). Additionally, we tracked cyanobacteria bloom dynamics and identified indicator species in both lakes. *Microcystis* and *Anabaena/Dolichospermum* blooms exhibited a conserved microbiome irrespective of the basin of origin or date. This suggests that the proposed interactome for *Microcystis* could be applied for other bloom-forming species. However, the transient nature of the *Anabaena/Dolichospermum* blooms in Lake George hindered the assessment of its microbiome' dynamics, if any, and suggest that future research should include an intensive sampling before bloom' senescence. Crucially, extending the monitoring before the onset of the bloom season in Chautauqua Lake is necessary to assess cyclical changes and repeatable patterns that can be used to fuel early warnings models of ecosystem transitions (Ortiz et al., 2020) or to predict blooms in long term studies (Tromas et al., 2017). Finally, access to the molecular tools and personnel required for a rapid turnaround or blooms is limited. In this context, the advantages of the sequencing technology presented in this study became particularly compelling, especially for researchers in resource-limited settings where access to expensive sequencers remains a significant constraint.

CRediT authorship contribution statement

Manuel Castro Berman: Writing – review & editing, Writing – original draft, Methodology, Investigation, Formal analysis, Data curation, Conceptualization. **Allison R. Hrycik:** Writing – review & editing. **Angelica Costello:** Writing – review & editing, Methodology. **Yang Bai:** Writing – review & editing, Methodology, Data curation. **Kevin C. Rose:** Writing – review & editing, Project administration, Funding acquisition, Conceptualization. **Rick Relyea:** Writing – review & editing, Funding acquisition. **Jonathan S. Dordick:** Writing – review & editing, Writing – original draft, Supervision, Resources, Funding acquisition, Conceptualization.

Declaration of competing interest

The authors declare that they have no known competing financial interests or personal relationships that could have appeared to influence the work reported in this paper.

Data availability

Data will be made available on request.

Acknowledgments

Funding was provided by The Jefferson Project at Lake George, which is a collaboration of Rensselaer Polytechnic Institute, IBM Research, the Lake George Association, and the Chautauqua Institution. In addition to funding from the four partners, the Lake George sensor network was supported by NSF MRI grant number 1625044 to RR, KCR, and 8 others and New York State Higher Education Capital grant number 7290 to RR. KCR was supported with funding from NSF grants 1754265 and 2048031. We are grateful to Brian Mattes and Candace Schermerhorn for assistance with sample collection and Laurie E. Ahrens for water quality analyses. MCB wants to thank Dr. M.E. Llames from INTECH for providing feedback on the initial draft of the manuscript, as well as three anonymous reviewers whose input improved the manuscript.

Appendix A. Supplementary data

Supplementary data to this article can be found online at https://doi.org/10.1016/j.ecolind.2024.111738.

References

Adams, H.E., Crump, B.C., Kling, G.W., 2014. Metacommunity dynamics of bacteria in an arctic lake: The impact of species sorting and mass effects on bacterial production and biogeography. Front. Microbiol. 5, 1–10. https://doi.org/10.3389/fmicb.2014.00082.

Al-Tebrineh, J., Pearson, L.A., Yasar, S.A., Neilan, B.A., 2012. A multiplex qPCR targeting hepato- and neurotoxigenic cyanobacteria of global significance. Harmful Algae 15, 19–25. https://doi.org/10.1016/j.hal.2011.11.001.

Baird, D.J., Hajibabaei, M., 2012. Biomonitoring 2.0: A new paradigm in ecosystem assessment made possible by next-generation DNA sequencing. Mol. Ecol. 21, 2039–2044. https://doi.org/10.1111/j.1365-294X.2012.05519.x.

Bockwoldt, K.A., Nodine, E.R., Mihuc, T.B., Shambaugh, A.D., Stockwell, J.D., 2017. Reduced Phytoplankton and Zooplankton Diversity Associated with Increased Cyanobacteria in Lake Champlain, USA. J. Contemp. Water Res. Educ. 160, 100–118. https://doi.org/10.1111/j.1936-704x.2017.03243.x.

Bogard, M.J., Vogt, R.J., Hayes, N.M., Leavitt, P.R., 2020. Unabated Nitrogen Pollution Favors Growth of Toxic Cyanobacteria over Chlorophytes in Most Hypereutrophic Lakes. https://doi.org/10.1021/acs.est.9b06299.

Brown, K., 2022. Investigation into the Environmental Drivers of Microcystin and Saxitoxin Production in Harmful Algal Blooms in Chautauqua Lake. Bowling Green State University, Bowling Green State University, NY.

Bruns, N.E., Heffernan, J.B., Ross, M.R.V., Doyle, M., 2022. A simple metric for predicting the timing of river phytoplankton blooms. Ecosphere 13, 1–8. https://doi.org/10.1002/ecs2.4348.

Buelo, C.D., Carpenter, S.R., Pace, M.L., 2018. A modeling analysis of spatial statistical indicators of thresholds for algal blooms. Limnol. Oceanogr. Lett. 3, 384–392. https://doi.org/10.1002/lol2.10091.

Burton, A.S., Stahl, S.E., John, K.K., Jain, M., Juul, S., Turner, D.J., Harrington, E.D., Stoddart, D., Paten, B., Akeson, M., Castro-Wallace, S.L., 2020. Off Earth Identification of Bacterial Populations Using 16S rDNA Nanopore Sequencing. Genes (basel). 11, 76. https://doi.org/10.3390/genes11010076.

Butitta, V.L., Carpenter, S.R., Loken, L.C., Pace, M.L., Stanley, E.H., 2017. Spatial early warning signals in a lake manipulation. Ecosphere 8. https://doi.org/10.1002/ecs2.1941.

Cai, H., Jiang, H., Krumholz, L.R., Yang, Z., 2014. Bacterial community composition of size-fractioned aggregates within the phycosphere of cyanobacterial blooms in a eutrophic freshwater lake. PLoS One 9. https://doi.org/10.1371/journal.pone.0102879.

Cao, K.A.L., Costello, M.E., Lakis, V.A., Bartolo, F., Chua, X.Y., Brazeilles, R., Rondeau, P., 2016. MixMC: A multivariate statistical framework to gain insight into microbial communities. PLoS One 11. https://doi.org/10.1371/journal.pone.0160169.

Carmichael, W.W., 2001. Health Effects of Toxin-Producing Cyanobacteria: "The CyanoHABs". Hum. Ecol. Risk Assess. an Int. J. 7, 1393–1407. https://doi.org/10.1080/20018091095087.

Carpenter, S.R., Arani, B.M.S., Hanson, P.C., Scheffer, M., Stanley, E.H., Van Nes, E., 2020. Stochastic dynamics of Cyanobacteria in long-term high-frequency observations of a eutrophic lake. Limnol. Oceanogr. Lett. 5, 331–336. https://doi.org/10.1002/lol2.10152.

Caruso, G., La Ferla, R., Azzaro, M., Zoppini, A., Marino, G., Petochi, T., Corinaldesi, C., Leonardi, M., Zaccone, R., Fonda Umani, S., Caroppo, C., Monticelli, L., Azzaro, F., Decembrini, F., Maimone, G., Cavallo, R.A., Stabili, L., Hristova Todorova, N.K., Karamfilov, V., Rastelli, E., Cappello, S., Acquaviva, M.I., Narracci, M., De Angelis, R., Del Negro, P., Latini, M., Danovaro, R., 2016. Microbial assemblages for environmental quality assessment: Knowledge, gaps and usefulness in the European Marine Strategy Framework Directive. Crit. Rev. Microbiol. 42, 883–904. https://doi.org/10.3109/1040841X.2015.1087380.

Castro Berman, M., Llames, M.E., Minotti, P., Fermani, P., Quiroga, M.V., Ferraro, M.A., Metz, S., Zagarese, H.E., 2020. Field evidence supports former experimental claims on the stimulatory effect of glyphosate on picocyanobacteria communities. Sci. Total Environ. 701, 134601 https://doi.org/10.1016/j.scitotenv.2019.134601.

Castro Berman, M., O' Farrell, I., Huber, P., Marino, D., Zagarese, H., 2022. A large-scale geographical coverage survey reveals a pervasive impact of agricultural practices on plankton primary producers. Agric. Ecosyst. Environ. 325, 107740 https://doi.org/10.1016/j.agee.2021.107740.

Clarke, K.R., Warwick, R.M., 1994. Similarity-based testing for community pattern: the two-way layout with no replication. Mar. Biol. 118, 167–176. https://doi.org/10.1007/BF00699231.

Cook, K.V., Li, C., Cai, H., Krumholz, L.R., Hambright, K.D., Paerl, H.W., Steffen, M.M., Wilson, A.E., Burford, M.A., Grossart, H.P., Hamilton, D.P., Jiang, H., Sukenik, A., Latour, D., Meyer, E.I., Padisák, J., Qin, B., Zamor, R.M., Zhu, G., 2020. The global Microcystis interactome. Limnol. Oceanogr. 65, S194–S207. https://doi.org/10.1002/lno.11361.

Cordier, T., Alonso-Sáez, L., Apothéloz-Perret-Gentil, L., Aylagas, E., Bohan, D.A., Bouchez, A., Chariton, A., Creer, S., Frühe, L., Keck, F., Keeley, N., Laroche, O., Leese, F., Pochon, X., Stoeck, T., Pawlowski, J., Lanzén, A., 2021. Ecosystems monitoring powered by environmental genomics: A review of current strategies with an implementation roadmap. Mol. Ecol. 30, 2937–2958. https://doi.org/10.1111/mec.15472.

Cui, Y., Chun, S.J., Ko, S.R., Lee, H.G., Srivastava, A., Oh, H.M., Ahn, C.Y., 2017. Reyranella aquatilis sp. Nov., an alphaproteobacterium isolated from a eutrophic lake. Int. J. Syst. Evol. Microbiol. 67, 3496–3500. https://doi.org/10.1099/ijsem.0.002151.

De Cáceres, M., Legendre, P., 2009. Associations between species and groups of sites: Indices and statistical inference. Ecology 90, 3566–3574. https://doi.org/10.1890/08-1823.1.

Dray, S., Legendre, P., Blanchet, G., 2009. packfor: Forward Selection with permutation (Canoco p. 46). R Packag. version 0.0-7/r58.

Dreher, T.W., Collart, L.P., Mueller, R.S., Halsey, K.H., Bildfell, R.J., Schreder, P., Sobhakumari, A., Ferry, R., 2019. Anabaena/Dolichospermum as the source of lethal microcystin levels responsible for a large cattle toxicosis event. Toxicon X 1, 100003. https://doi.org/10.1016/j.toxcx.2018.100003.

Eiler, A., Bertilsson, S., 2004. Composition of freshwater bacterial communities associated with cyanobacterial blooms in four Swedish lakes. Environ. Microbiol. 6, 1228–1243. https://doi.org/10.1111/j.1462-2920.2004.00657.x.

Gerphagnon, M., Macarthur, D.J., Latour, D., Gachon, C.M.M., Van Ogtrop, F., Gleason, F.H., Sime-Ngando, T., 2015. Microbial players involved in the decline of filamentous and colonial cyanobacterial blooms with a focus on fungal parasitism. Environ. Microbiol. 17, 2573–2587. https://doi.org/10.1111/1462-2920.12860.

Guo, D., Liang, J., Chen, W., Wang, J., Ji, B., Luo, S., 2020. Bacterial community analysis of two neighboring freshwater lakes originating from one lake. Polish J. Environ. Stud. 30, 111–117. https://doi.org/10.15244/pjoes/119094.

Ha, J.H., Hidaka, T., Tsuno, H., 2009. Quantification of toxic microcystis and evaluation of its dominance ratio in blooms using real-time PCR. Environ. Sci. Technol. 43, 812–818. https://doi.org/10.1021/es801265f.

Hintz, W.D., Schuler, M.S., Borrelli, J.J., Eichler, L.W., Stoler, A.B., Moriarty, V.W., Ahrens, L.E., Boylen, C.W., Nierzwicki-Bauer, S.A., Relyea, R.A., 2020. Concurrent improvement and deterioration of epilimnetic water quality in an oligotrophic lake over 37 years. Limnol. Oceanogr. 65, 927–938. https://doi.org/10.1002/lno.11359.

Hotto, A.M., Satchwell, M.F., Berry, D.L., Gobler, C.J., Boyer, G.L., 2008. Spatial and temporal diversity of microcystins and microcystin-producing genotypes in Oneida Lake, NY. Harmful Algae 7, 671–681. https://doi.org/10.1016/j.hal.2008.02.001.

Hu, H., Jin, D., Yang, Y., Zhang, J., Ma, C., Qiu, Z., 2021. Distinct profile of bacterial community and antibiotic resistance genes on microplastics in Ganjiang River at the watershed level. Environ. Res. 200, 111363 https://doi.org/10.1016/j.envres.2021.111363.

Jiang, L., Yang, L., Xiao, L., Shi, X., Gao, G., Qin, B., 2007. Quantitative studies on phosphorus transference occuring between Microcystis aeruginosa and its attached bacterium (Pseudomonas sp.). Hydrobiologia 581, 161–165. https://doi.org/10.1007/s10750-006-0518-0.

Jüttner, F., Watson, S.B., 2007. Biochemical and Ecological Control of Geosmin and 2-Methylisoborneol in Source Waters. Appl. Environ. Microbiol. 73, 4395–4406. https://doi.org/10.1128/AEM.02250-06.

Koeppel, A.F., Goodrum, W., Steffen, M., Turner, S.D., 2022. Environmental DNA sequencing data from algal blooms in Lake Erie using Oxford Nanopore MinION. https://doi.org/10.1101/2022.03.12.483776.

Komárek, J., 2016. A polyphasic approach for the taxonomy of cyanobacteria: principles and applications. Eur. J. Phycol. 51, 346–353. https://doi.org/10.1080/09670262.2016.1163738.

Kratzer, C.R., Brezonik, P.L., 1981. A Carlson-Type Trophic State Index for nitrogen in Florida lakes. JAWRA J. Am. Water Resour. Assoc. 17, 713–715. https://doi.org/10.1111/j.1752-1688.1981.tb01282.x.

Lê Cao, K.A., Boitard, S., Besse, P., 2011. Sparse PLS discriminant analysis: Biologically relevant feature selection and graphical displays for multiclass problems. BMC Bioinformatics 12. https://doi.org/10.1186/1471-2105-12-253.

Lee, S.J., Jang, M.H., Kim, H.S., Yoon, B.D., Oh, H.M., 2000. Variation of microcystin content of Microcystis aeruginosa relative to medium N: P ratio and growth stage. J. Appl. Microbiol. 89, 323–329. https://doi.org/10.1046/j.1365-2672.2000.01112.x.

Lefler, F.W., Berthold, D.E., Laughinghouse, H.D., 2023. Cyanoseq: A database of cyanobacterial 16S rRNA gene sequences with curated taxonomy. J. Phycol. 59, 470–480. https://doi.org/10.1111/jpy.13335.

Legendre, P., Gallagher, E.D., 2001. Ecologically meaningful transformations for ordination of species data. Oecologia 129, 271–280. https://doi.org/10.1007/s004420100716.

Li, H., 2018. Sequence analysis Minimap2 : pairwise alignment for nucleotide sequences 34, 3094–3100. https://doi.org/10.1093/bioinformatics/bty191.

Lindström, E.S., Bergström, A.K., 2004. Influence of inlet bacteria on bacterioplankton assemblage composition in lakes of different hydraulic retention time. Limnol. Oceanogr. 49, 125–136. https://doi.org/10.4319/lo.2004.49.1.0125.

Logue, J.B., Lindström, E.S., 2010. Species sorting affects bacterioplankton community composition as determined by 16S rDNA and 16S rRNA fingerprints. ISME J. 4, 729–738. https://doi.org/10.1038/ismej.2009.156.

López-Archilla, A.I., Moreira, D., López-García, P., Guerrero, C., 2004. Phytoplankton diversity and cyanobacterial dominance in a hypereutrophic shallow lake with biologically produced alkaline pH. Extremophiles 8, 109–115. https://doi.org/10.1007/s00792-003-0369-9.

Mankiewicz-Boczek, J., Font-Nájera, A., 2022. Temporal and functional interrelationships between bacterioplankton communities and the development of a toxigenic Microcystis bloom in a lowland European reservoir. Sci. Rep. 12, 1–15. https://doi.org/10.1038/s41598-022-23671-2.

Mather, K.F., 1939. Physiography of Eastern United States . By Nevin M. Fenneman. 691 pp., maps, photographs and diagrams, index. New York: McGraw-Hill Book Company. 1938. $6.00. Science (80-.). 90, 493–493. https://doi.org/10.1126/science.90.2343.493.a.

Matsuo, Y., Komiya, S., Yasumizu, Y., Yasuoka, Y., Mizushima, K., Takagi, T., Kryukov, K., Fukuda, A., Morimoto, Y., Naito, Y., Okada, H., Bono, H., Nakagawa, S., Hirota, K., 2021. Full-length 16S rRNA gene amplicon analysis of human gut microbiota using MinION^{TM} nanopore sequencing confers species-level resolution. BMC Microbiol. 21, 1–14. https://doi.org/10.1186/s12866-021-02094-5.

McDonald, K.E., Lehman, J.T., 2013. Dynamics of Aphanizomenon and Microcystis (cyanobacteria) during experimental manipulation of an urban impoundment. Lake Reserv. Manag. 29, 103–115. https://doi.org/10.1080/10402381.2013.800172.

McKindles, K.M., Manes, M.A., DeMarco, J.R., McClure, A., McKay, R.M., Davis, T.W., Bullerjahn, G.S., 2020. Dissolved Microcystin Release Coincident with Lysis of a Bloom Dominated by Microcystis spp. in Western Lake Erie Attributed to a Novel Cyanophage. Appl. Environ. Microbiol. 86 https://doi.org/10.1128/AEM.01397-20.

Meslier, V., Quinquis, B., Da Silva, K., Plaza Oñate, F., Pons, N., Roume, H., Podar, M., Almeida, M., 2022. Benchmarking second and third-generation sequencing platforms for microbial metagenomics. Sci. Data 9, 1–9. https://doi.org/10.1038/s41597-022-01762-z.

Methe, B.A., Hiorns, W.D., Zehr, J.P., 1998. Contrasts between marine and freshwater bacterial community composition: Analyses of communities in Lake George and six other Adirondack lakes. Limnol. Oceanogr. 43, 368–374. https://doi.org/10.4319/lo.1998.43.2.0368.

Miller, T.R., Beversdorf, L., Chaston, S.D., McMahon, K.D., 2013. Spatiotemporal Molecular Analysis of Cyanobacteria Blooms Reveals Microcystis-Aphanizomenon Interactions. PLoS One 8, e74933. https://doi.org/10.1371/journal.pone.0074933.

Niu, Y., Shen, H., Chen, J., Xie, P., Yang, X., Tao, M., Ma, Z., Qi, M., 2011. Phytoplankton community succession shaping bacterioplankton community composition in Lake Taihu. China. Water Res. 45, 4169–4182. https://doi.org/10.1016/j.watres.2011.05.022.

O'Neil, J.M., Davis, T.W., Burford, M.A., Gobler, C.J., 2012. The rise of harmful cyanobacteria blooms: The potential roles of eutrophication and climate change. Harmful Algae 14, 313–334. https://doi.org/10.1016/j.hal.2011.10.027.

Ortiz, D., Palmer, J., Wilkinson, G., 2020. Detecting changes in statistical indicators of resilience prior to algal blooms in shallow eutrophic lakes. Ecosphere 11. https://doi.org/10.1002/ecs2.3200.

Paerl, H.W., Havens, K.E., Hall, N.S., Otten, T.G., Zhu, M., Xu, H., Zhu, G., Qin, B., 2020a. Mitigating a global expansion of toxic cyanobacterial blooms: confounding effects and challenges posed by climate change. Mar. Freshw. Res. 71, 579. https://doi.org/10.1071/MF18392.

Paerl, H.W., Havens, K.E., Xu, H., Zhu, G., McCarthy, M.J., Newell, S.E., Scott, J.T., Hall, N.S., Otten, T.G., Qin, B., 2020b. Mitigating eutrophication and toxic cyanobacterial blooms in large lakes: The evolution of a dual nutrient (N and P) reduction paradigm. Hydrobiologia 847, 4359–4375. https://doi.org/10.1007/s10750-019-04087-y.

Paerl, H.W., Otten, T.G., 2016. Duelling 'CyanoHABs': unravelling the environmental drivers controlling dominance and succession among diazotrophic and non-N 2 -fixing harmful cyanobacteria. Environ. Microbiol. 18, 316–324. https://doi.org/10.1111/1462-2920.13035.

Pernthaler, J., 2017. Competition and niche separation of pelagic bacteria in freshwater habitats. Environ. Microbiol. 19, 2133–2150. https://doi.org/10.1111/1462-2920.13742.

Pound, H.L., Martin, R.M., Sheik, C.S., Steffen, M.M., Newell, S.E., Dick, G.J., McKay, R.M.L., Bullerjahn, G.S., Wilhelm, S.W., 2021. Environmental Studies of Cyanobacterial Harmful Algal Blooms Should Include Interactions with the Dynamic Microbiome. Environ. Sci. Technol. https://doi.org/10.1021/acs.est.1c04207.

R.-Core-Team, 2022. R: A language and environment for statistical computing.

Reinl, K.L., Harris, T.D., North, R.L., Almela, P., Berger, S.A., Bizic, M., Burnet, S.H., Grossart, H., Ibelings, B.W., Jakobsson, E., Knoll, L.B., Lafrancois, B.M., McElarney, Y., Morales-Williams, A.M., Obertegger, U., Ogashawara, I., Paule-Mercado, M.C., Peierls, B.L., Rusak, J.A., Sarkar, S., Sharma, S., Trout-Haney, J.V., Urrutia-Cordero, P., Venkiteswaran, J.J., Wain, D.J., Warner, K., Weyhenmeyer, G.A., Yokota, K., 2023. Blooms also like it cold. Oceanogr. Lett. Limnol. https://doi.org/10.1002/lol2.10316.

Rozas, M., Brillet, F., Callewaert, C., Paetzold, B., 2022. MinIONTM Nanopore Sequencing of Skin Microbiome 16S and 16S–23S rRNA Gene Amplicons. Front. Cell. Infect. Microbiol. 11, 1–9. https://doi.org/10.3389/fcimb.2021.806476.

Ruka, A.T., Johansen, J.R., Leps, J., Loken, Z.J., Schuler, M., Mattes, B., Yates, E., Relyea, R.A., 2022. Seasonal diatom community responses to development and climate change in Lake George, an oligotrophic lake in the Adirondack Mountains. Hydrobiologia 849, 2761–2780. https://doi.org/10.1007/s10750-022-04892-y.

Sagova-Mareckova, M., Boenigk, J., Bouchez, A., Cermakova, K., Chonova, T., Cordier, T., Eisendle, U., Elersek, T., Fazi, S., Fleituch, T., Frühe, L., Gajdosova, M., Graupner, N., Haegerbaeumer, A., Kelly, A.M., Kopecky, J., Leese, F., Nõges, P., Orlic, S., Panksep, K., Pawlowski, J., Petrusek, A., Piggott, J.J., Rusch, J.C., Salis, R., Schenk, J., Simek, K., Stovicek, A., Strand, D.A., Vasquez, M.I., Vrålstad, T., Zlatkovic, S., Zupancic, M., Stoeck, T., 2021. Expanding ecological assessment by integrating microorganisms into routine freshwater biomonitoring. Water Res. 191, 116767 https://doi.org/10.1016/j.watres.2020.116767.

Sánchez, M.L., Izaguirre, I., Zagarese, H., Schiaffino, M.R., Castro Berman, M., Lagomarsino, L., Chaparro, G., Baliña, S., Vera, M.S., Cheruvelil, K.S., 2023. Drivers of planktonic chlorophyll a in pampean shallow lakes. Ecol. Indic. 146 https://doi.org/10.1016/j.ecolind.2022.109834.

Santos, A., van Aerle, R., Barrientos, L., Martinez-Urtaza, J., 2020. Computational methods for 16S metabarcoding studies using Nanopore sequencing data. Comput. Struct. Biotechnol. J. 18, 296–305. https://doi.org/10.1016/j.csbj.2020.01.005.

Scheffer, M., Hosper, S.H., Meijer, M.-L., Moss, B., Jeppesen, E., 1993. Alternative equilibria in shallow lakes. Trends Ecol. Evol. 8, 275–279. https://doi.org/10.1016/0169-5347(93)90254-M.

Sharma, G., Khatri, I., Subramanian, S., 2016. Complete Genome of the Starch-Degrading Myxobacteria Sandaracinus amylolyticus DSM 53668T. Genome Biol. Evol. 8, 2520–2529. https://doi.org/10.1093/gbe/evw151.

Sharma, M., Khurana, H., Singh, D.N., Negi, R.K., 2021. The genus Sphingopyxis: Systematics, ecology, and bioremediation potential - A review. J. Environ. Manage. 280, 111744 https://doi.org/10.1016/j.jenvman.2020.111744.

Smith, R.B., Bass, B., Sawyer, D., Depew, D., Watson, S.B., 2019. Estimating the economic costs of algal blooms in the Canadian Lake Erie Basin. Harmful Algae 87, 101624. https://doi.org/10.1016/j.hal.2019.101624.

Smith, Z.J., Conroe, D.E., Schulz, K.L., Boyer, G.L., 2020. Limnological Differences in a Two-Basin Lake Help to Explain the Occurrence of Anatoxin-a, Paralytic Shellfish Poisoning Toxins, and Microcystins. Toxins (basel). 12 https://doi.org/10.3390/toxins12090559.

Stainbrook, K., Ross, C., Davis, C., Townley, L., 2022. Developing a watershed screening tool to estimate relative contribution of phosphorus to guide management planning. J. Environ. Manage. 312, 114937 https://doi.org/10.1016/j.jenvman.2022.114937.

Swinton, M.W., Eichler, L.W., Farrell, J.L., Boylen, C.W., 2015. Evidence for water temperature increase in Lake George, NY: impact on growing season duration and degree days. Lake Reserv. Manag. 31, 241–253. https://doi.org/10.1080/10402381.2015.1067660.

Tanvir, R.U., Hu, Z., Zhang, Y., Lu, J., 2021. Cyanobacterial community succession and associated cyanotoxin production in hypereutrophic and eutrophic freshwaters. Environ. Pollut. 290, 118056 https://doi.org/10.1016/j.envpol.2021.118056.

Tromas, N., Fortin, N., Bedrani, L., Terrat, Y., Cardoso, P., Bird, D., Greer, C.W., Shapiro, B.J., 2017. Characterising and predicting cyanobacterial blooms in an 8-year amplicon sequencing time course. ISME J. 11, 1746–1763. https://doi.org/10.1038/ismej.2017.58.

Wacklin, P., Hoffmann, L., Komárek, J., 2009. Nomenclatural validation of the genetically revised cyanobacterial genus Dolichospermum (RALFS ex BORNET et FLAHAULT) comb. nova. Fottea 9, 59–64. https://doi.org/10.5507/fot.2009.005.

Wang, K., Mou, X., Cao, H., Struewing, I., Allen, J., Lu, J., 2021. Co-occurring microorganisms regulate the succession of cyanobacterial harmful algal blooms ☆. Environ. Pollut. 288, 117682 https://doi.org/10.1016/j.envpol.2021.117682.

Wang, H., Sivonen, K., Rouhiainen, L., Fewer, D.P., Lyra, C., Rantala-Ylinen, A., Vestola, J., Jokela, J., Rantasärkkä, K., Li, Z., Liu, B., 2012. Genome-derived insights into the biology of the hepatotoxic bloom-forming cyanobacterium Anabaena sp. strain 90. BMC Genomics 13, 613. https://doi.org/10.1186/1471-2164-13-613.

Wang, J., Wei, Z.P., Chu, Y.X., Tian, G., He, R., 2022. Eutrophic levels and algae growth increase emissions of methane and volatile sulfur compounds from lakes. Environ. Pollut. 306, 119435 https://doi.org/10.1016/j.envpol.2022.119435.

Werner, D., Acharya, K., Blackburn, A., Zan, R., Plaimart, J., Allen, B., Mgana, S.M., Sabai, S.M., Halla, F.F., Massawa, S.M., Haile, A.T., Hiruy, A.M., Mohammed, J., Vinitnantharat, S., Thongsamer, T., Pantha, K., Mota Filho, C.R., Lopes, B.C., 2022. MinION Nanopore Sequencing Accelerates Progress towards Ubiquitous Genetics in Water Research. Water 14, 2491. https://doi.org/10.3390/w14162491.

Wu, Y., Li, L., Zheng, L., Dai, G., Ma, H., Shan, K., Wu, H., Zhou, Q., Song, L., 2016. Patterns of succession between bloom-forming cyanobacteria Aphanizomenon flos-aquae and Microcystis and related environmental factors in large, shallow Dianchi Lake, China. Hydrobiologia 765, 1–13. https://doi.org/10.1007/s10750-015-2392-0.

Yang, Y., Chen, J., Chen, X., Jiang, Q., Liu, Y., Xie, S., 2021. Cyanobacterial bloom induces structural and functional succession of microbial communities in eutrophic lake sediments. Environ. Pollut. 284, 117157 https://doi.org/10.1016/j.envpol.2021.117157.

Zhao, Y., Luo, M., Zhou, Y., Jia, X., Kang, S., Yang, S., Mu, Q., 2022. Spatial patterns of dominant bacterial community components and their influential factors in the southern Qinling Mountains. China. Front. Microbiol. 13, 1–14. https://doi.org/10.3389/fmicb.2022.1024236.

Zhu, C., Zhang, J., Nawaz, M.Z., Mahboob, S., Al-Ghanim, K.A., Khan, I.A., Lu, Z., Chen, T., 2019. Seasonal succession and spatial distribution of bacterial community structure in a eutrophic freshwater Lake. Lake Taihu. Sci. Total Environ. 669, 29–40. https://doi.org/10.1016/j.scitotenv.2019.03.087.